Light Trapping using Anisotropic Plasmonic Nanoparticles

A thesis submitted towards the fulfilment of the BS-MS Dual Degree Program

By

Kavya S S

(20121048)

Under the guidance of

Prof. Sulabha K Kulkarni (Supervisor)

and

Dr. G V Pavan Kumar (Co-supervisor)

Indian Institute of Science Education and Research (IISER) Pune

Certificate

This is to certify that this dissertation entitled "*Light trapping using anisotropic plasmonic nanoparticles*" towards the partial fulfilment of the BS-MS dual degree programme at the Indian Institute of Science Education and Research, Pune represents study/work carried out by **Kavya S S** at IISER Pune under the supervision of **Prof. Sulabha K Kulkarni** and **Dr. G V Pavan Kumar** during the academic year 2016-2017.

Kavya S S

Registration number : 20121048

Dr. G V Pavan Kumar (Co-supervisor)

Assistant Professor

Committee

Prof. Sulabha K Kulkarni (supervisor)

Dr. G V Pavan Kumar (co-supervisor)

Dr. Ashna Bajpai (TAC)

30/03/17

Declaration

I hereby declare that the matter embodied in the report entitled " Light trapping using anisotropic plasmonic nanoparticles" are the results of the work carried out by me at the Department of Physics, IISER, Pune, under the supervision of Prof. Sulabha K Kulkarni and Dr. G V Pavan Kumar and the same has not been submitted elsewhere for any other degree.

Kavya S S

Registration Number : 20121048

30/03/17

Dr. G V Pavan Kumar (Co-supervisor)

Assistant Professor

Dedicated to my family

Acknowledgements

Firstly, I would like to express my sincere gratitude to my research advisor Prof. Sulabha K Kulkarni for guiding me throughout the project with her immense knowledge, continuous support and constant encouragement. I would like to express my heartiest gratitude to our collaborator Prof. Manoj Namboothiri of IISER Trivandrum for his valuable suggestions and experimental advices throughout and Dr. G V Pavan Kumar for taking the responsibility to be my Co-supervisor and for the constant and sincere support from time to time. I am thankful to Dr. Smita Chaturvedi on her helpful supports and suggestions. I am also thankful to my lab mates Abhijit, Harjot, Swathi, Jithin, and Chaitanya for keeping a pleasant lively lab atmosphere, their cooperation and open discussions.

I, sincerely thank Dr. Rane of CMET Institute for helping me with the transmission electron microscopy measurements, Dr. Pramod Pillai for letting me use the solid state spectrophotometer, Dr. Ashana Bajpai for the conductivity measurements and Anil Prathamshetti and Yatish for helping me on acquiring all the FESEM data. I am also grateful to the department of science and technology (DST), for the INSPIRE scholarship for financial support. Finally I thank each and every scientific and administrative staff of IISER, Pune for helping directly or indirectly with this work.

Contents

List of Figures

Abstract

The urge for a renewable energy source to take over the conventional fossil energy sources has always been a necessity. Thus a lot of work and effort has been spend on the photovoltaic cell research which focuses on conversion of solar energy into electrical energy. The studies in this field so far had classified the photovoltaic cells into first, second and third generation cells with the common single crystalline silicon solar cells being the first generation, thin film solar cells are the second generation and third generations consists of nanocrystalline materials, polymer materials, perovskite materials or some hybrid materials which give hopes on a cost effective as well as efficient production of a photovoltaic cell. Basically third generation solar cells are not limited by the Schottky-Queisser limit of power efficiency and can be efficient beyond even ~90%. This however, is yet a dream and not realized so far in any practical solar cell fabricated. Attempts are therefore made to improve the photovoltaic cells using different concepts.

In this project attempt is to investigate the effect of different shapes and sizes of the gold/silver nanoparticles on trapping the light since efficient trapping of light is needed to increase the cell efficiency. Gold and silver nanoparticles exhibit absorption of electromagnetic radiation in the visible part of the electromagnetic spectrum known as Localized Surface Plasmon Resonance (LSPR). The use of anisotropic nanoparticles like rods, tetrapods, triangles, stars, cubes etc. have size and shape dependent much broader absorption properties which can extend in the visible range to IR, the part of the solar spectrum which in most of the cases is not possible to use. One can also make alloy plasmonic structures which also can affect the absorption favourably to improve the performance.

In this project, nanoparticles of spherical, rod, stars, cubes and cage shapes of gold and silver were synthesized and their characterization was performed using UV-Visible spectrophotometer and FESEM. Then they are introduced into the widely used conductive polymer PEDOT:PSS (Poly(3,4-ethylenedioxythiophene)-poly(styrenesulfonate)) and their optical and electrical properties in solution and thin film are studied for measuring their light trapping efficiency

CHAPTER 1

INTRODUCTION

With the beginning of gold nanoparticle synthesis by Michael Faraday, nanoscience and technology came so far exploring the "plenty of room at the bottom."

As we know 'nano' explores studies of materials with at least one of the dimensions is in the size range of 1-100 nm (1nm = 10^{-9} m). These materials with high surface to volume ratio show interesting optical, electrical and mechanical properties. These unusual properties made high expectation from nanotechnology in different sectors. One among them is of course the energy sector. By reports of world energy council till 2015, the main source of energy consumption is still from Oil with ~ 33%, then coal giving ~ 29%, gas ~24%, nuclear fuels ~4% , hydro ~7% and the rest 3% is constituted by renewable energy sources such as wind, solar etc. A rapid development for low cost, large scale and long term sustaining energy source has become a strong necessity.

In a year around 12,000 TW energy from sun strikes on earth. But no major breakthrough has been found so far on tapping this solar energy which could power up the whole world unlimited without putting any life on danger. From 1839 with the discovery of photovoltaic effect by French scientist A E Becquerel and the fabrication of first solar cell on 1883 by Charles Fritts with 1% efficiency, research on photovoltaic cell had been a hot topic on making cells of higher efficiency with lower cost. Coming through various generations of photovoltaic cells, today we are keeping our hopes on nanomaterials for an efficient cell.

This project work is mainly focussed on understanding the light trapping abilities of the nanoparticles made of two materials gold and silver by manipulating their plasmonic properties through different shapes and sizes. Both isotropic and anisotropic particles are made in both the materials for comparison by materials, size and shape.

1.1 Plasmonic materials

Metals are abundant in free electrons with an electron density of 10^{22} to 10^{23} /cm^3. So considering these electrons together we talk about dielectric confinement in metals. The collective response of these electrons to electromagnetic radiation is studied under the name plasmonics.

Mie theory is one of the very first theories to discuss the interaction of electromagnetic waves with small spherical particles[1]. With the help of Maxwell's equations Mie could explain the reduction in intensity observed for incident electromagnetic waves when they are allowed to pass through a medium containing small spherical particles of same size. When electromagnetic radiation of a particular intensity Io and wavelength λ is allowed to pass through a medium with spherical particles embedded uniformly the reduced intensity I can be calculated using D'Lambert equation.

$$I = Ioe^{-\mu x} \qquad (1)$$

Where extinction coefficient, $\mu = \frac{N}{VC_{ext}}$ N is the number of particles in the medium, V-volume of the colloidal particles and C is the extinction coefficient, which is the sum of absorption and scattering coefficients.

According to Mie theory, in the case of smaller particles of radius R, where absorption contributes more to extinction coefficient,

$$C_{ext} = \frac{24\pi^2 R^3 \varepsilon_m^{\frac{3}{2}}}{\lambda} \frac{\varepsilon_2^2}{(\varepsilon_1+2\varepsilon_m)^2+\varepsilon_2^2} \qquad (2)$$

Here ε is the dielectric constant of particles which can be written as $\varepsilon = \varepsilon_1 + \varepsilon_2$ and ε_m is that of the medium.

From equation 2, one of the conditions for a maximal absorption is

$$\varepsilon_1 = -2\varepsilon_m \qquad (3)$$

Which give rise to the strong resonance band.

It is to be noted that C_{ext} is zero when ε_2 is zero or ε_2 is infinity. But Mie theory could not explain the dependence of size of the particles on absorption.

A better description of this idea is given in Drude model.

Consider an electromagnetic wave on a metal nanoparticle. The electrons in the particle will have a collective oscillatory response to the electric field of the applied wave.

Let the electric field *be* $E = E_o e^{-i\omega t}$ (4)

Where ω is the frequency of the wave and E_o be the amplitude of electric field.

Then the equation of motion for the collective response of the electrons are given classically by

$$m\frac{d^2x}{dt^2} + \gamma\frac{dx}{dt} + m\omega_o^2 x = eE_o e^{-i\omega t} \quad (5)$$

Where the γ in the damping term is the reciprocal of relaxation time of an electron. Solving equation 5 gives

$$x = \frac{eE/m}{\omega_0^2 - \omega^2 - i\omega_d\omega} \quad (6)$$

Where ω_d is the damping frequency, given by γ/m.

Now the collective response can produce a net polarisation, and proceeding with further substitutions gives an important parameter can be reached, called plasma frequency

$$\omega_p = \sqrt{\frac{Ne^2}{\varepsilon_o m_e}} \quad (7)$$

Where N is the number of electrons per unit volume, and m_e is the mass of electron. This is an indication of coherency with which electrons are oscillating in an applied electromagnetic radiation. For the nanoparticles, their characters are mainly governed by the surface effects and thus surface plasmons have a major role in deciding the optical and electrical properties of metal nanoparticles.

These collective response of electrons in a conductive nanoparticle, when it's size is less than the wavelength of the applied electromagnetic wave give rise to the optical phenomenon

known as localised surface plasmon resonance (LSPR) effect. Frequency of this oscillation being a function of composition, morphology, size, dielectric environment and separation distance of particles each nanoparticle sample gives rise to a characteristic LSPR effect which is analysed for their characterizations.

1.2 Photovoltaic cells

The basic working of a photovoltaic cell is the absorption of solar energy, generation of electrons and capturing the ejected electrons in order to create a flow of electrons in an outside circuit.

Photovoltaic cells are generally divided into three categories, first, second and third generation cells. First generation photovoltaic cells consists of silicon based cells. They consist of large areas of monocrystalline or polycrystalline silicon p-n junctions. Even though they approach the theoretical efficiency of 33% in light harvesting[2], the high cost of production suggested the needs for alternatives which lead to second generation of photovoltaic cells. They are thin films of crystalline or amorphous silicon which are much cheaper compared to the first generation solar cells in construction. But these cells had stability issues possibly due to bad contacts, sensitivity towards atmospheric components such as moisture, oxygen etc. Also their light harvesting efficiency fell way below that of first generation solar cells. Then came along the third generation photovoltaic cells which are modified in material, composition, layer stacking etc. and they are of organic, inorganic or hybrid in nature. They are flexible and can exceed the Schockley-Queisser limit of 33% efficiency, hence can turn out to be more economical. They make use of semiconductor quantum dots, polymer or smaller molecules, perovskites etc. for light absorption. In fact today's trend is to invoke newer materials and ideas so that solar cells with better efficiency and stability are possible in future.

Briefly touching on the working of photovoltaic cells, silicon based ones are more established as we said earlier. In a thin layer of silicon wafer both n type and p type materials such as phosphorous and boron respectively are doped. Thus at the junction of their meeting they create a charge free area called a p-n junction or depletion region which results in electrical imbalance at the two sides of the junction. This results into an electric field at the junction. When photons of sunlight strike the cell, the electric field created at the junction can provide

both direction and momentum for the generated electrons. The created electrons flow is taken to an external circuit.

Here the extent of the use of complete solar spectrum is limited as only the photons with energy higher than the band gap of the absorbing material can excite the electrons in a single junction photovoltaic cells. Introduction of different materials such that their difference in band gaps can be manipulated to use most of the solar spectrum is called multi junction photo voltaic cells. Gallium arsenide cells are one of the examples of multi junction cells and they were able to attain an efficiency of up to 35% today[3].

The applications of photovoltaic cells vary from power stations, telecommunications signalling to source power for space crafts. The high demand for this renewable energy source harvesting made research in this field rapid and more efficient leading to exploring different methods on improving the current cell efficiency or the use of new materials.

Here we discuss only organic photovoltaic cell.

1.3 Organic photovoltaic cell

Organic photovoltaic cells are the topic of interest today as they are very cheap and easy to fabricate compared to the silicon based cells. Organic cells itself is comprised of three types of cells, semiconducting polymer based, two polymers of electron donating and electron accepting ones based and bulk hetero junction devices in which these two types of polymers are mixed together. The third one is preferred to be of a better advantage, as exciton diffusion length is really short and on creation of electro hole pair they might recombine before reaching the interface of donor and acceptor layers. For an efficient absorption of sunlight the active layer must be at least 100 nm which is much larger than the exciton diffusion length of 10-20nm[4].

A usual OPVC consists of electrodes, buffer layer, donor and acceptor layers.

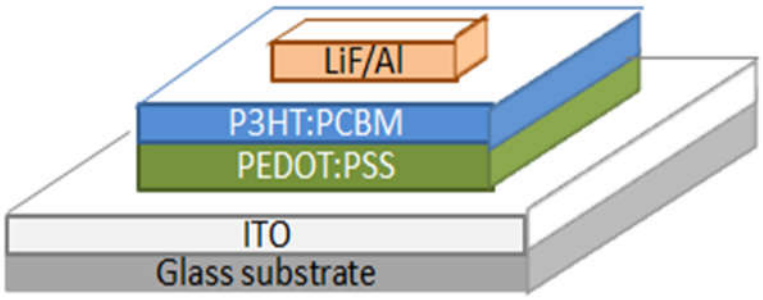

Figure 1.1 : Schematic diagram of a typical organic photovoltaic cell, Adapted from[5]

For a typical OPVC its working stages are shown below

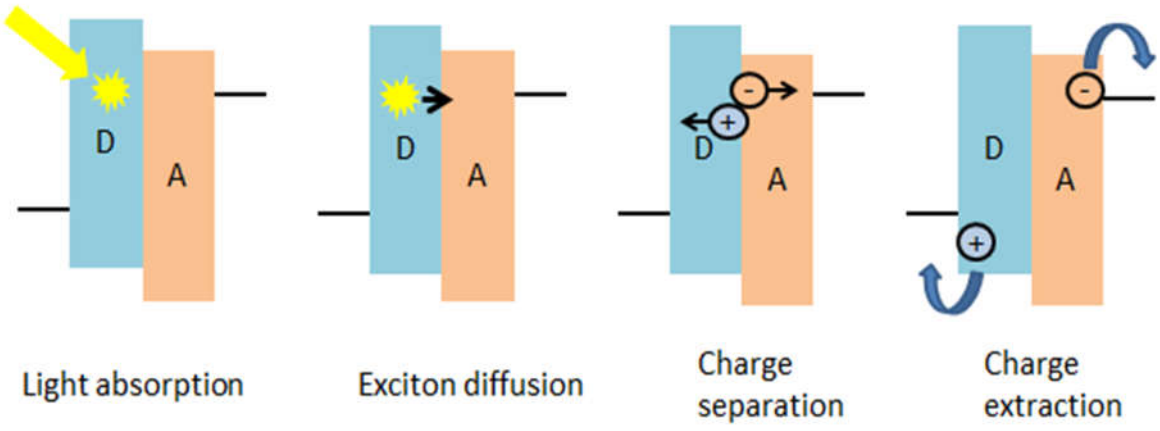

Figure 1.2 : Schematic diagram for the working of a photovoltaic cell, Adapted from[6]

A successful candidate of OPV cell of bulk hetero junction (BHJ) type with polymer-fullerene combination of photo active layer has already managed to score a power conversion efficiency of more than 8% by now[7].

Various ways have been tried so far to increase the photon absorption efficiency of OPVC. Introduction of new low band gap polymers, increasing the active layer thickness, use of inorganic optical spacer in between active layer and electrode, introduction of plasmonic nanoparticles etc.[8]. In these plasmonic nanoparticle incorporation is considered to be better compared to others as they are effective, simple to process and can be easily tuned to excite different modes by simply modifying their shapes and size.

Metal nanoparticles of gold, silver etc. shows intense localised surface plasmon resonance effect which can be used to increase the light absorption efficiencies of the OPVC. These particles can increase the light absorption by intensifying the electromagnetic field near the nanoparticles and scattering light on surface by increasing the optical thickness of the layer. More the scattering more the chance for the light to be trapped within the film of the cell which can in turn cause the generation of more exciton pairs leading to an increase in the efficiency[7].

Now the question has to be addressed to which layer of the OPVC these nanoparticles has to be embedded in order to get the highest efficiency. There are three ways in which it can be done. First one is the introduction of NPs into the photo active layer of the OPVC, but here it is observed to quench the excitons and thus decrease the photon conversion efficiency. Second way is the introduction of NPs between the ITO electrode and buffer layer, but this step requires vacuum deposition of metal monolayer and thermal treatments afterwards. The third and the most welcomed way today is the incorporation of NP into the buffer layer of the cell, where some of the particles can be extended to photo active layer also thus extending the LSPR effects and reducing the overall device resistance. Smaller nanoparticles (5-20nm) are better light absorbers compared to the larger nanoparticles (>50nm) which can couple and trap propagating plane waves into the next active layer[7].

The buffer layer used here is a highly conductive polymer PEDOT:PSS (Poly(3,4-ethylenedioxythiophene)-poly(styrenesulfonate)). It provides as a hole conducting layer which can improve the surface roughness of the substrate and at the same time provide a good electrical contact between the ITO anode and the photoactive layer. It also improves the work function of the ITO layer[7].

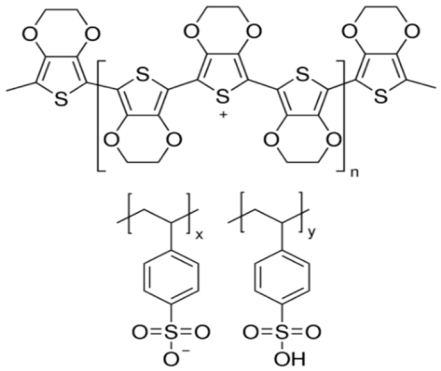

Figure 1.3 : Chemical structure of the polymer PEDOT:PSS[8]

Plasmonic materials are introduced into the PEDOT:PSS layers, where PEDOT is the conductive polymer and PSS is doped with it which can act as a surfactant. This blend keeps the transparency high throughout the UV-Visible spectrum. No absorption maximum is found between 400-800 nm range. The light trapped by means of wide angle scattering of the entered light into the active layer thus increases the light path length within the cell volume. Some studies are showing that more than the LSPR effects increased hole transport efficiency and decreased exciton quenching can lead to higher absorption. The incorporated nanoparticles can induce both morphological and chemical changes in the PEDOT:PSS layer which can also be a contributing factor[9].

.

1.4 Summary

Application of nanoparticles in the energy sector has been a topic of interest since a long time as finding a renewable source of energy for the increased energy demands has been a difficult task. By using nanomaterials in photovoltaic cells, scientists are trying to achieve a long term, efficient and economically feasible solution to the energy crisis.

Coming through the generations of photovoltaic cells with the crystalline silicon p-n junction to the use of polymer mixed organic photovoltaic cells, efficiency and cost of production are compromised alternatively. But with the third generation of photo voltaic cells now, lots of research is focussed on increasing the efficiency by the incorporation of nanoparticles into the layers of the cell.

In this study nanoparticles of two different materials, gold and silver are made in order to compare their role in the PEDOT:PSS layer of photo voltaic cell in increasing their light absorption efficiency. Different shapes such as spheres, rods, cubes and stars are made in order to differentiate the effects of isotropic (sphere) nanoparticle to anisotropic nanoparticles in this role. Also the difference in sizes also in the corresponding shapes can help on reaching a conclusion on tuning the LSPR peaks to the desired range of spectrum.

For the characterisation of materials synthesized, UV-Visible spectrophotometer, field emission scanning electron microscopy, transmission electron microscopy, conductivity measurements are used.

CHAPTER 2

EXPERIMENTAL TECHNIQUES

In order to find out the effect of nanoparticles on organic photo voltaic cells, particles of different shapes and sizes such as spheres, rods, cubes and stars were synthesized of metal nanoparticles of both gold and silver following chemical routes. The localized surface plasmon resonance of these materials is used to manipulate the absorption of regular PEDOT:PSS polymer buffer layer in the cells.

2.1 Chemicals and Materials

Chloroauric acid ($HAuCl_4$. $3H_20$), Cetyltrimethyl ammonium bromide (CTAB), Sodium citrate , Sodium borohydride ($NaBH_4$), Ascorbic acid ,Benzyl dodecyl dimethyl ammonium chloride (BDAC), Copper chloride ($CuCl_2.2H_2O$), Glucose, Hexadecyl amine (HDA), Polyvinyl pyrollidone (PVP), Polyethylene glycol (PEG), Silver nitrate ($AgNO_3$),), Sodium sulphide (Na_2S), Poly(3,4-ethylenedioxythiophene) polystyrene sulfonate (PEDOT:PSS) were purchased from Sigma Aldrich of analytical grade. Ethylene glycol (EG), Acetone, Isopropyl alcohol, Ethanol purchased of laboratory grade. Distilled water.

2.2 Synthesis

2.2.1 Gold nanospheres

This is done as a three step process. In the first, 0.01M, 0.25 ml $HAuCl_4$ and 0.01 M Sodium citrate solution is added to 9.5 ml distilled water and the resulting solution is homogeneously mixed. 0.1 M, 0.3 ml reducing agent $NaBH_4$ is added to the above mixture, resulting in a pink colour solution. These citrate stabilized gold nanoparticles are kept undisturbed for 3 hours after they are mixed by rapid inversion. In the second step , 45 ml , 0.08 M CTAB (Cetyltrimethyl ammonium bromide) and 0.01 M $HAuCl_4$ is added to 0.25 ml , 0.1 M ascorbic acid solution which then mixed by gentle inversion . Then 5 ml of the above citrate capped seed solution is introduced to this mixture resulting in 8 nm spherical gold

nanoparticles .In the third part, the same mixture of CTAB, $HAuCl_4$ and ascorbic acid is made and then 5 ml of above 8 nm spherical particles are introduced, which is mixed for 10 minutes and kept undisturbed for next 3 hours for the formation of gold nanospheres ~ 20nm[10].

2.2.2 Gold nanorods

The seed solution comprises of 0.2 M , 5 ml CTAB , 0.5 mM , 5 ml $HAuCl_4$ to which freshly prepared ice cold $NaBH_4$ is added under vigorous stirring , resulting in a brownish yellow colour solution. For the growth solution, 0.2 M, 2.5 ml CTAB is mixed with 0.15 M, 2.5 ml BDAC (Benzyl dodecyl dimethyl ammonium chloride) and 4 mM, 0.2 ml $AgNO_3$, then added to $HAuCl_4$ 1 mM, 5 ml solution with gentle mixing. After that 0.0788 M, 0.07 ml weak reducing agent ascorbic acid is added with shaking which turns the solution colourless. 20 µl of the seed solution is added to the growth solution and kept overnight for the formation of gold nanorods ~ 40 nm long[11].

2.2.3 Gold - Copper nanostars

0.5 ml 0f 100 mM $HAuCl_4$ and $CuCl_2$ is mixed with 0.47 ml 0f 1M glucose . This mixture is added to 6.5 ml H_2O with hexadecylamine. The solution is stirred for 24 hours at room temperature. After that, it is kept at 100^oC in an oil bath for 40 minutes with continuous stirring. Nanostars of 200 nm are formed by this procedure[12].

2.2.5 Gold nanocages

0.25 ml of Silver nanocubes solution is diluted up to 1 ml using distilled water. To the above PVP (1ml, 1mM), ascorbic acid (0.01 ml, 0.1mM) , CTAB (1ml, 20mM) are added. Under stirring 0.3 ml of 1mM $HAuCl_4$ is added at a rate of 25 µl per minute. Stirring is continued for another 30 minutes[13].

2.2.6 Silver nanospheres

444 mg of PVP (molecular weight – 40K) is added to 40 ml of polyethylene glycol solution with stirring at 80^oC. When the solution becomes transparent in colour, 1 ml of 0.5 M aqueous $AgNO_3$ solution is rapidly injected into it. When the reaction attains light yellow colour, it is transferred into 80 ml teflon container autoclave for 24 hours in 260^oC, resulting in the formation of spherical particles of ~50 nm diameter[14].

2.2.7 Silver nanocubes

2.2.7.1 Cubes – 190nm

5 ml of anhydrous ethylene glycol is heated at 160°C for 1 hour in order to remove the water content. 3 ml ethylene glycol solutions of 0.25 M $AgNO_3$ and 0.375 M PVP-55 are added simultaneously at a rate of 0.375 ml/min. Heating is continued for next 45 minutes making ~ 190 nm sized cubes[15].

2.2.7.2 Cubes – 50nm

Pipette 6 ml ethylene glycol to a 20 ml vial and heat it for 1 hour. Meanwhile, 30 mg PVP-55 solution is made in 1.5 ml ethylene glycol and 24 mg $AgNO_3$ in 0.5 ml ethylene glycol and 0.3 mM solution of Na_2S is also prepared in ethylene glycol. After 1 hour of heating, 80µl of Na_2S solution is added. Then in 8-9 minutes, 1.5 ml of PVP solution is pipetted into the heating mixture. Immediately after this, 0.5 ml $AgNO_3$ solution is added. Reaction will be completed in 10-15 minutes giving silver nanocubes of 50 nm edge length[16].

2.3 Incorporating NPs into Polymer

The nanoparticles synthesized above of different shapes and sizes of materials gold and silver dispersed in distilled water are added in different volume to volume ratios of highly conductive PEDOT:PSS (poly(3,4-ethylenedioxythiophene) polystyrene sulfonate) polymer and blended thoroughly under ultra sonication for around two hours[17].

2.4 Thin film fabrication

For the construction of the thin film of PEDOT:PSS with the nanoparticles, first the ITO coated glasses are cleaned according the standard procedure followed commonly. For that the ITO coated glasses were cleaned by ultra sonicating using detergent for 20 minutes, distilled water for 30 minutes and in acetone and isopropyl alcohol for 20 minutes respectively. Then the slides are dried overnight at 120°C under vacuum. Later they are exposed to UV-Ozone treatment for 10 minutes before spin coating the blended solution of PEDOT:PSS with plasmonic nanoparticles[18].

2.5 Analysis techniques

2.5.1 UV-Vis Absorption spectroscopy

According to the Beer-Lambert's law, when an absorbing sample is exposed to electromagnetic radiation of intensity Io , the decrease in the intensity of the transmitted radiation, I is proportional to the concentration of the sample (c) and sample length (ℓ).

$$Log\left(\frac{I}{I_o}\right) = -\varepsilon c\ell \quad (8)$$

I/Io being the transmittance, absorbance, $A = \varepsilon c\ell$ (9)

In the Perkin Elmer Lambda 950 spectrophotometer used here, Figure 2.1

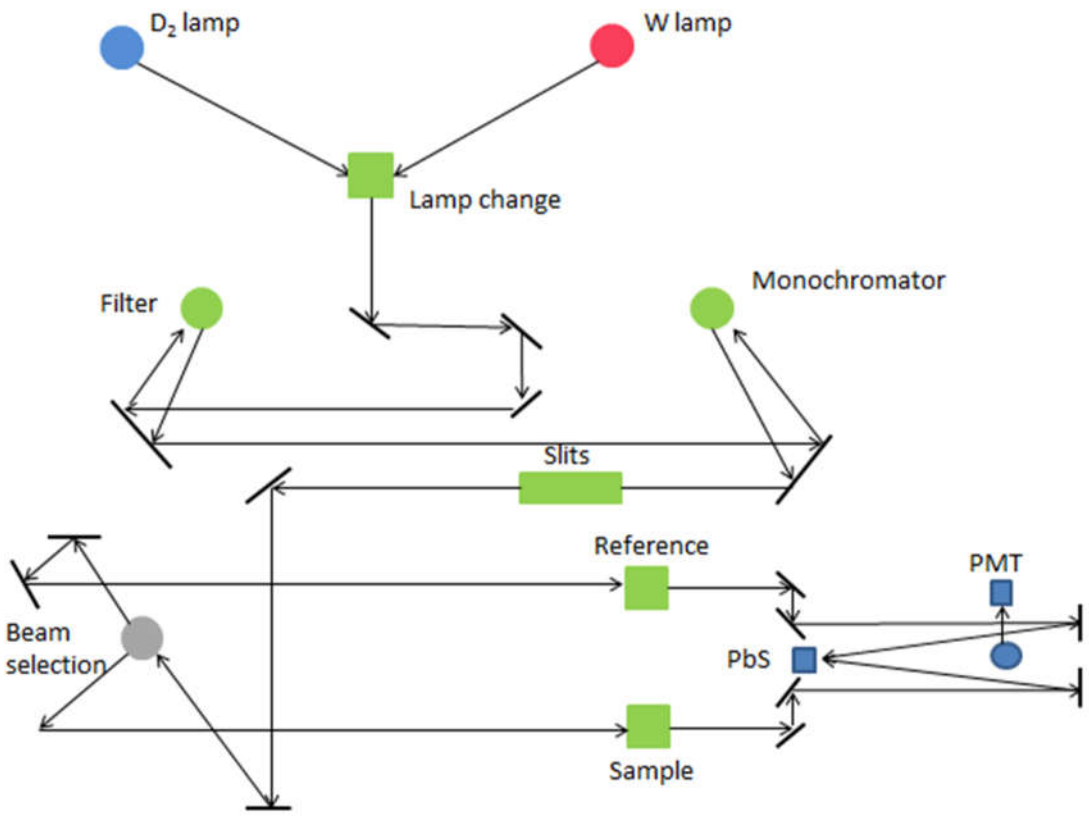

Figure 2.1 : Schematic diagram on the working of UV-Visible spectrophotometer

A hydrogen-deuterium lamp is used for the Ultraviolet region (till 320nm) and tungsten lamp for visible-Infra red region. From there monochromator selects particular wavelengths out of the incident polychromatic radiation to pass through the cuvettes which are made of quartz as

they do not absorb in the ultraviolet-visible-infrared region of the spectrum. A reference cuvette consisting the solvent used for dispersing nanoparticles is set to 100% transmission/0% absorption. When the radiation is allowed to pass through the sample electrons in their ground state absorbs the wavelengths corresponding to their energy gaps for the excitation of electrons to higher state. The radiations transmitted through the sample are detected using a photomultiplier tube and in case of infrared radiation lead sulphide is used for detection. For liquid samples they are directly taken in the cuvette for the measurement, but for the solid ones they are either made into a thin film or pellets for the measurements. The results are generated as a plot with wavelength against absorption/transmission/reflectance according to preference.

2.5.2 Field Emission Scanning Electron Microscopy

On a comparison of electron microscopy with optical microscopy, as the name suggests instead of electromagnetic radiations electron beams are used here, which provides a desired wavelength range due to the ability to tune the energies of electrons as seen from equation 10

$$\lambda = \frac{h}{\sqrt{2mE}} \qquad (10)$$

and optical lenses are replaced by the electromagnetic lenses for the focussing in case of electrons. The back scattered electrons helps to make out the morphology (size and shape) of the particles present in the sample. So only conducting samples can be analysed under SEM as insulating ones get charged due to incident electrons. But the insulated samples can also be studied by SEM by coating a thin layer of a conducting material generally gold, by techniques like sputtering. Here the source of electrons is through field emission and not hot cathodes, thus the name field emission scanning electron microscope.

In order to avoid complexities arising from slowing down and scattering of electrons by the collision with air molecules and at the same time to avoid oxidation and contamination of filament and samples are housed inside a vacuum chamber with 10^{-2} – 10^{-3} Pa pressure maintained inside.

Sample to be examined are sonicated or vortexed properly in order to disperse the particles properly in the solvent and ~ 10µl of the same is drop casted on a cleaned silica wafer and dried under vacuum before observed through scanning electron microscopy.

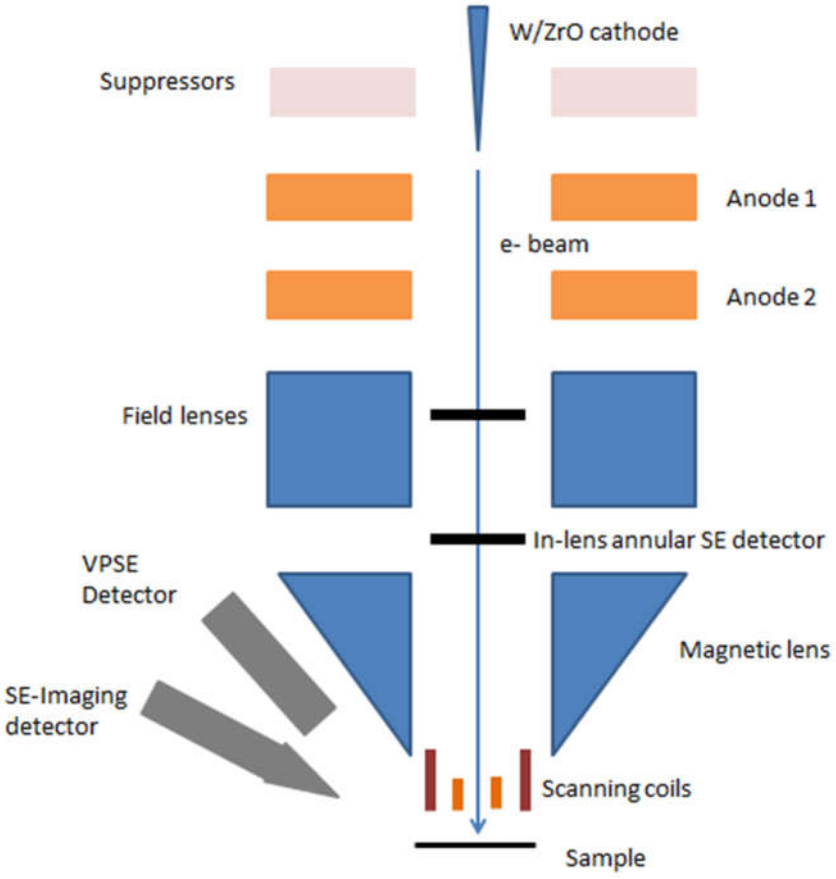

Figure 2.2 : Schematic diagram on the working of ZEISS Gemini FESEM

2.5.3 Spin coating

For the preparation of thin films ranging from nanometre to micrometre scale range on suitable substrates, spin coating method is adopted. Here the desired sample is mixed with an ink/polymer before casting on a substrate. Then the substrate is rotated at a suitable rotations per minute in which majority of the solvent is lost leaving an even film on the substrate. On drying the thin film under vacuum at a particular temperature, solvent evaporates.

In general the thin film thickness is inversely proportional to the angular velocity as

$$t \propto \frac{1}{\sqrt{\omega}}$$

It also depends on material concentration and evaporation rate of solvent. For this project I have used static dispense spin coating technique where solution is already drop casted before starting spinning compared to dynamic spin coating technique where the solution is casted while the spinning goes on.

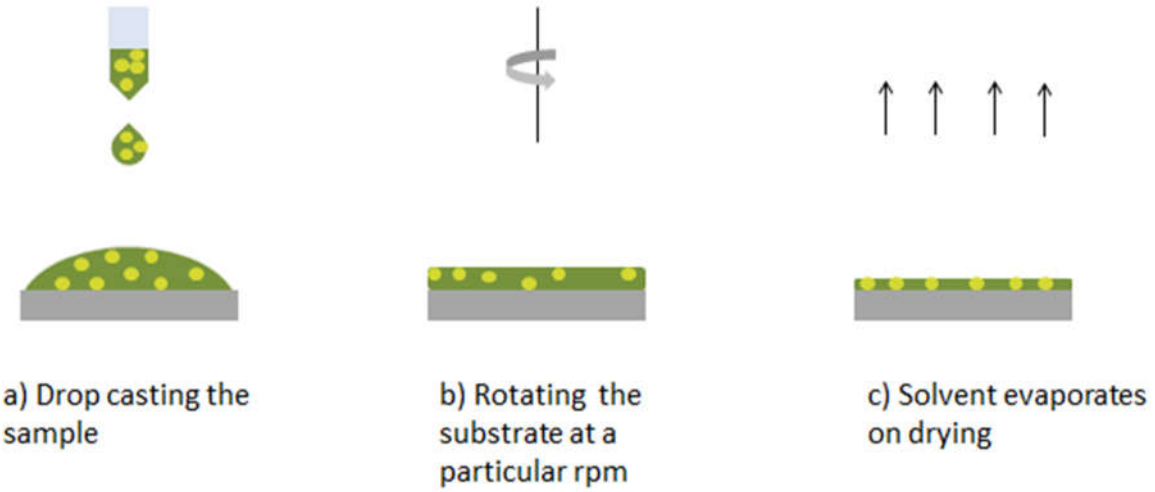

Figure 2.3 : Schematic diagram on the working of a spin coater

2.5.4 Transmission Electron Microscopy

The first transmission electron microscope was built way back in 1931 by Ernst Ruska and Max Knoll. Ruska was awarded the Nobel Prize for the development of TEM.

Compared to scanning electron microscope, instead of observing the scattered electrons from the sample, here the high energy electrons are allowed to pass through the sample and records the image. Typically electrons of energy > 50 keV are focussed into the sample by using series of electromagnetic lenses in order to achieve a resolution better than 0.5 nm. A typical setup includes electron source, condenser lens, specimen, objective lens, diffraction lens, intermediate lens, projector lens and fluorescent screen in order. These have to be kept in high vacuum of 10^{-3} to 10^{-4} Pa.

Here sample preparation has to be more careful compared to SEM, as it should be thin sample of not more than ~ 100 nm. It is possible to obtain diffraction images also using TEM

for the analysis of crystal structure which can be used to figure out size dependant lattice parameter change along with the defects in the structure.

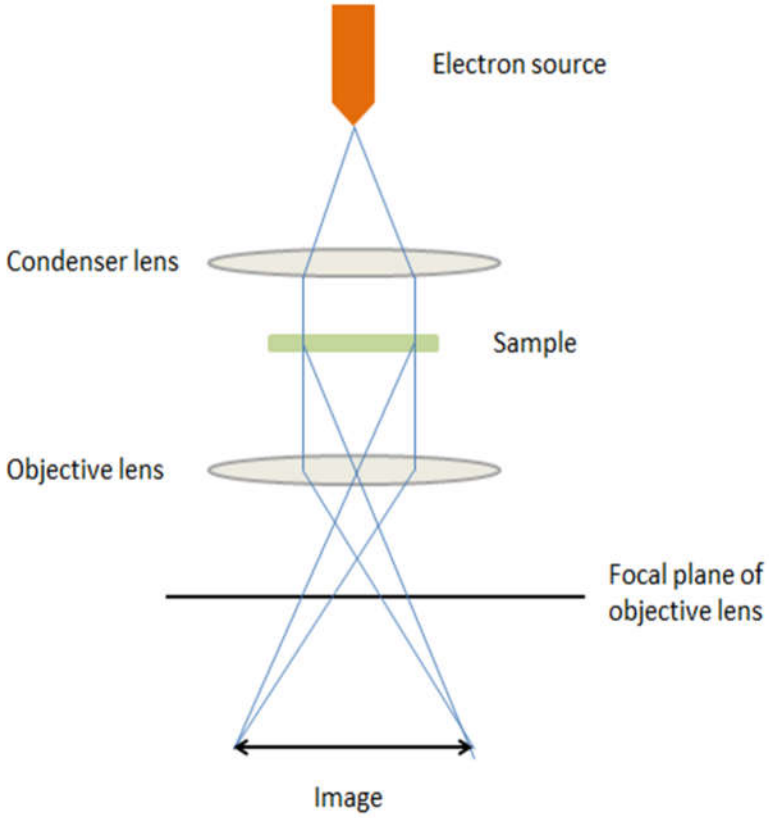

Figure 2.4 : Schematics of the working of transmission electron microscopy (TEM), adapted from[19]

CHAPTER 3

RESULTS AND DISCUSSION

In this chapter the results obtained for the synthesis followed for various shapes and sizes of gold and silver are discussed along with their properties measured when they were incorporated into the polymer PEDOT:PSS (Poly(3,4-ethylenedioxythiophene) polystyrene sulfonate) for the application to organic photovoltaic cells. Thin films are fabricated with the PEDOT:PSS nanoparticle mixture for each morphology, size and material for the comparison on their role in increasing the efficiency of photovoltaic cells.

3.1 Characterization

The nanoparticles of gold and silver synthesized following the procedures discussed in chapter 2 are analysed using the characterisation tools such as ultraviolet-visible-near infrared absorption spectroscopy, field emission scanning electron microscopy (FESEM) and dynamic light scattering.

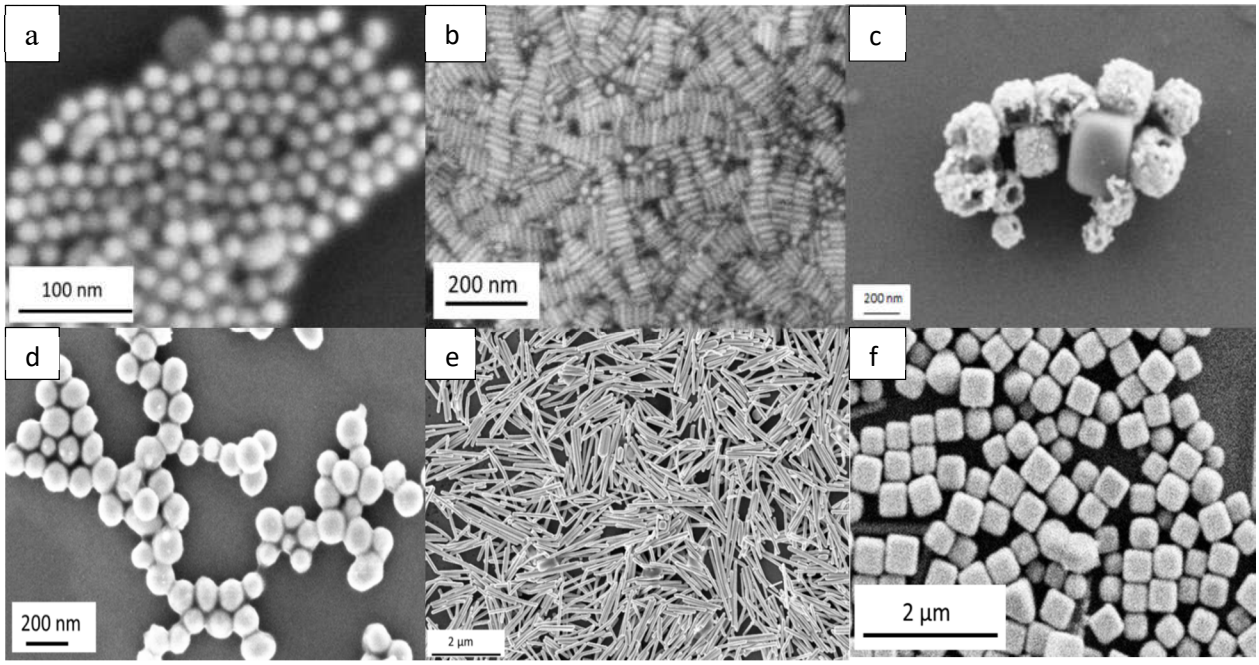

Figure 3.1 : FESEM images of gold a) spheres, b) rod, c) cage and silver d) sphere, e) rod and f) cubes

3.1.1 Gold nanospheres

Gold nanospheres made by following the seed mediated growth method as discussed in the previous chapter produced monodispersed sample. The magenta coloured sample under ultraviolet-visible irradiation in spectrophotometer gave a peak for localised surface plasmon resonance (LSPR) at around 524 nm.

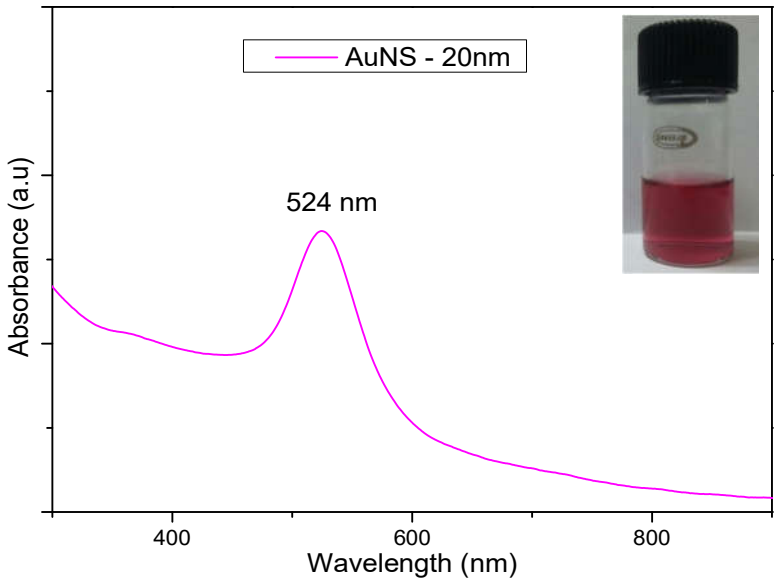

Figure 3.2 : UV-Visible spectrum of AuNS with inset image of the sample

The sample observed under FESEM showed that nanoparticles were indeed spherical in shape with a diameter of around 20 nm. Figure 3.3 shows the SEM images where it confirms the morphology to be spherical and ensures the monodispersity of the spherical sample over a large scale.

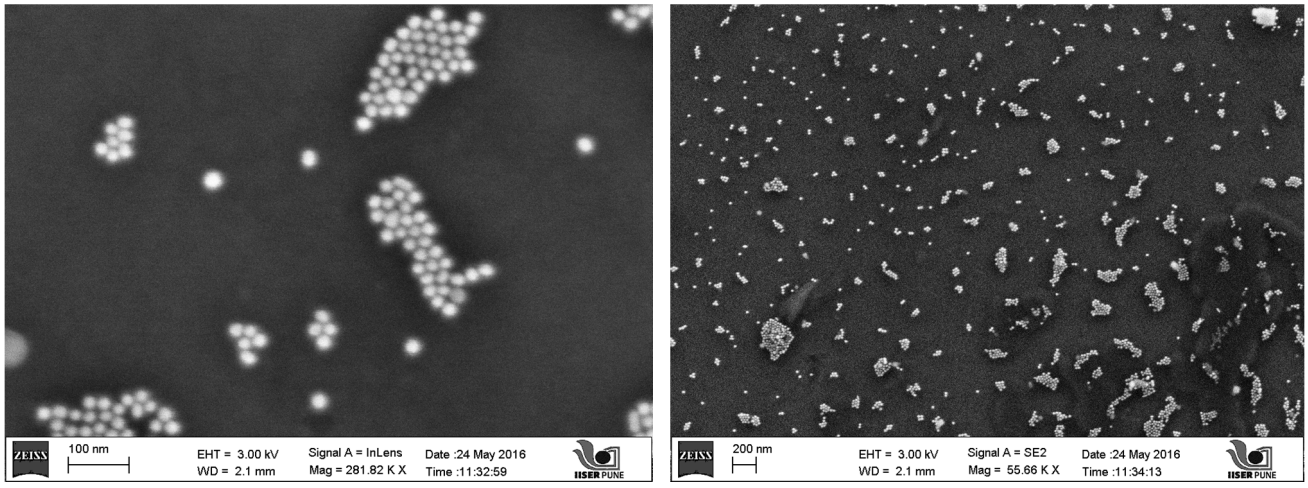

Figure 3.3 : FESEM Images of AuNS

3.1.2 Gold nanorods

The gold nanorods also followed by seed mediated growth method produced a highly monodisperse sample of around 40 nm length. Transverse and longitudinal modes of vibration of electrons in rod shaped nanoparticles gives these localised surface plasmon resonance peaks, here at 524 nm and 880 nm respectively.

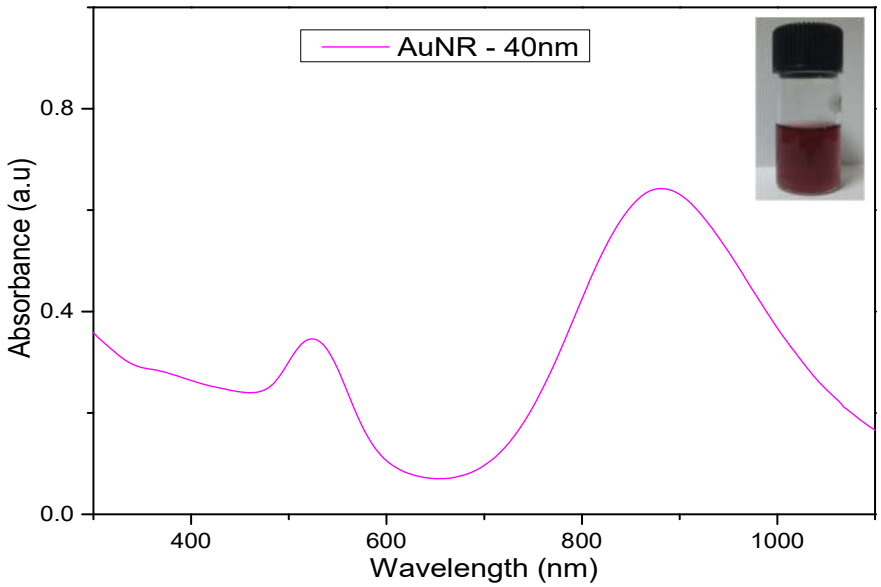

Figure 3.4 : UV-Vis spectrum of gold nanorods with inset picture of the sample

FESEM images of the sample shown below in Figure 3.5 confirm the morphology to be rods and second image shows the monodispersity over a wide scale.

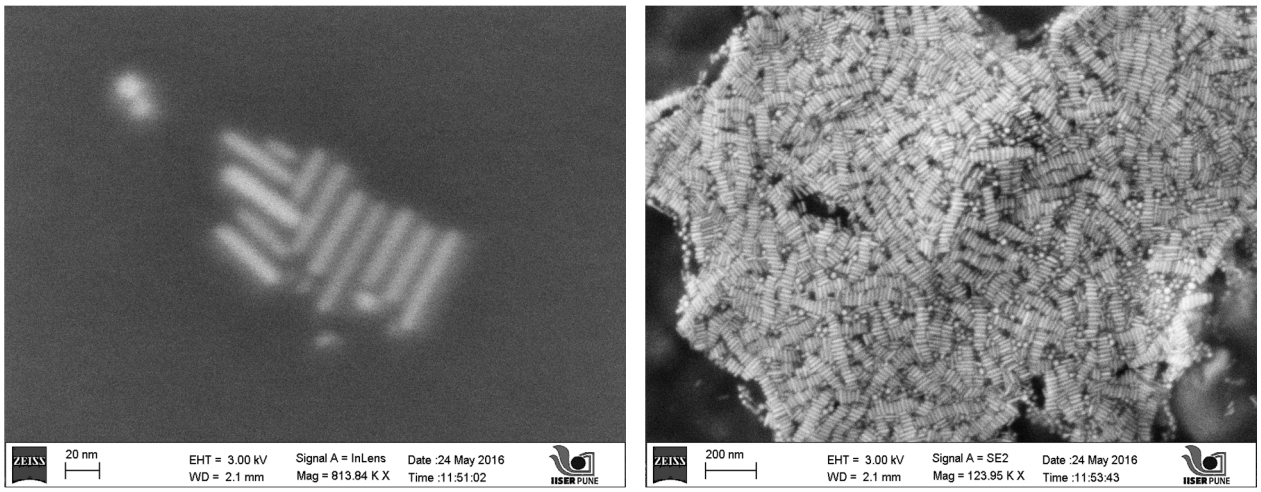

Figure 3.5 : FESEM Images of AuNRs

3.1.3 Gold – Copper nanostars

Pentagonal gold nanostars of 200 nm arm to arm length have been synthesized following the synthesizing procedure discussed before. The LSPR Peaks for the gold-copper sample were seen at 830 nm and 1270 nm.

.

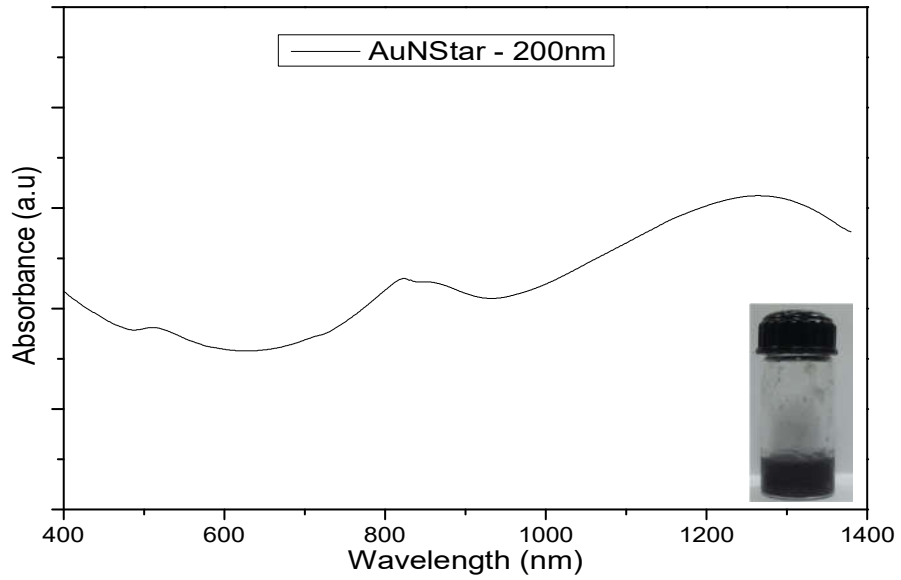

Figure 3.6 : UV-Vis spectrum of Au-Cu nanostars with an inset image of the sample

FESEM images of the sample shown below shows the pentacle stars of around 200 nm arm to arm length morphology and their distribution over a wide range ensuring the monodispersity of the sample used for further analysis.

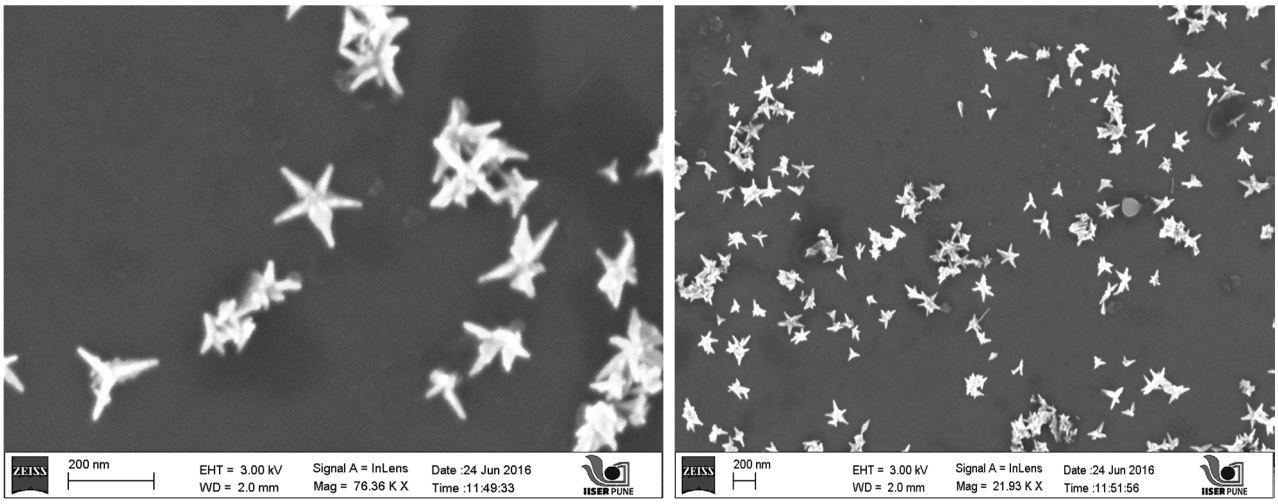

Figure 3.7 : FESEM Images of Au nanostars

3.1.4 Silver nanospheres

Silver nanospheres were synthesized according to polyol process discussed in chapter 2. Even though the procedures claimed to have uniform nanospheres of 50 nm size, synthesizing them keeping all other parameter constant and same gave the spheres to be average 120 nm in size. The UV-Visible absorption spectrum for the given sample showed a LSPR peak at 390 nm.

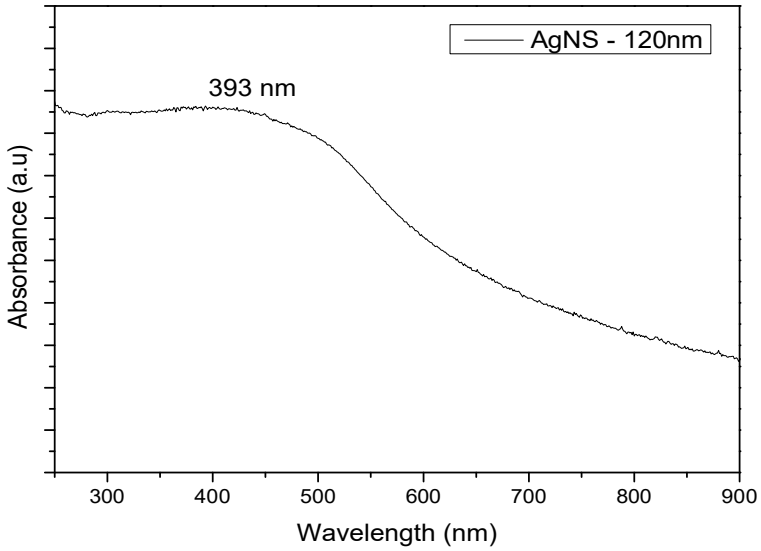

Figure 3.8 : UV-Visible spectrum of Ag nanospheres with inset image of sample

FESEM Images taken for the colloidal solution shows the silver spheres to have a size of average 120 nm. The morphology is maintained over a large scale.

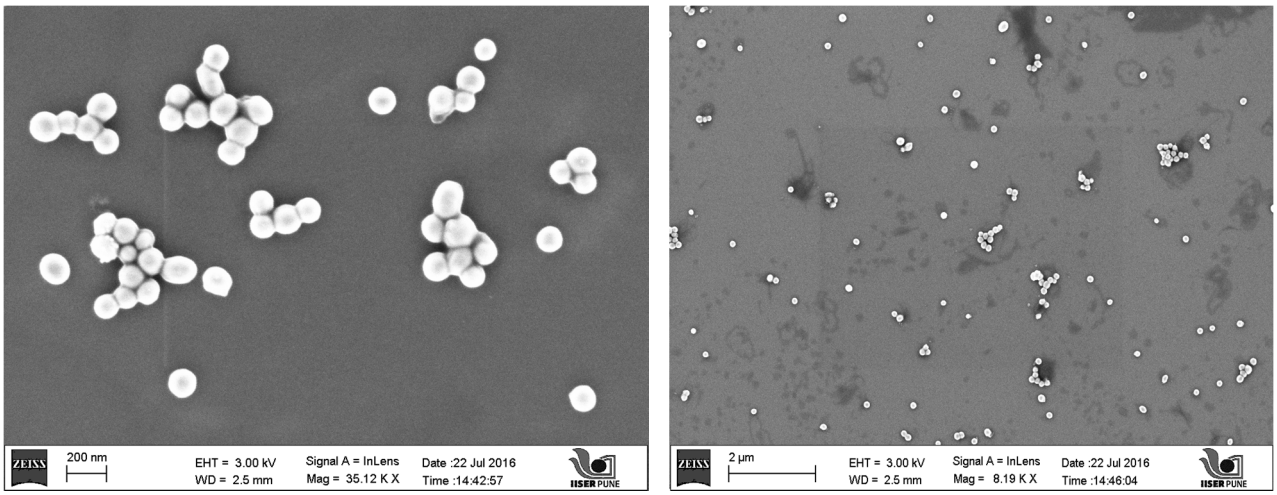

Figure 3.9 : FESEM Images of Ag nanospheres

3.1.5 Silver nanocubes

Silver nanocubes were synthesized following a polyol procedure as discussed in chapter 2. Figure below shows the UV-Visible absorption spectrum of the cubes with a LSPR peak at 436 nm.

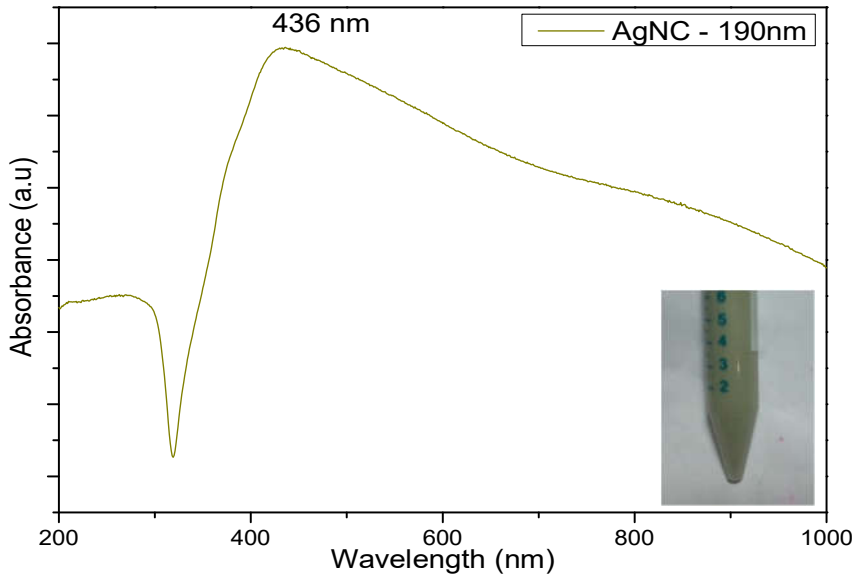

Figure 3.10 : UV-Vis absorption spectrum of Ag nanocubes with an inset image of sample

FESEM Images of the sample shown below gives the morphology to be cubes of around 190 nm in size.

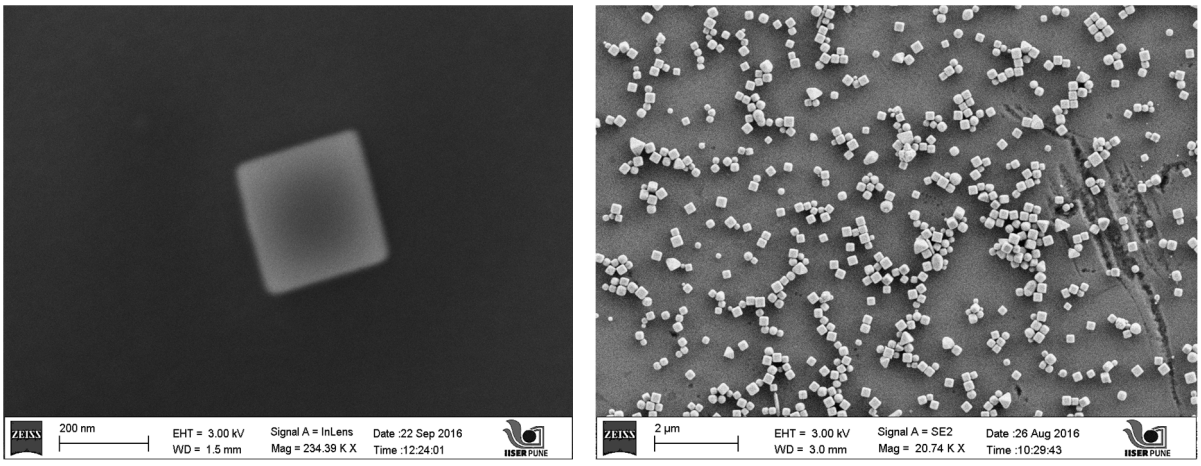

Figure 3.11 : FESEM Images of Ag nanocubes

Silver Cubes of 50 nm

A similar polyol process is followed for the synthesis of silver cubes of smaller size. UV-Visible absorption spectrum of the prepared sample of green ochre colour gives a similar LSPR peak at 424 nm.

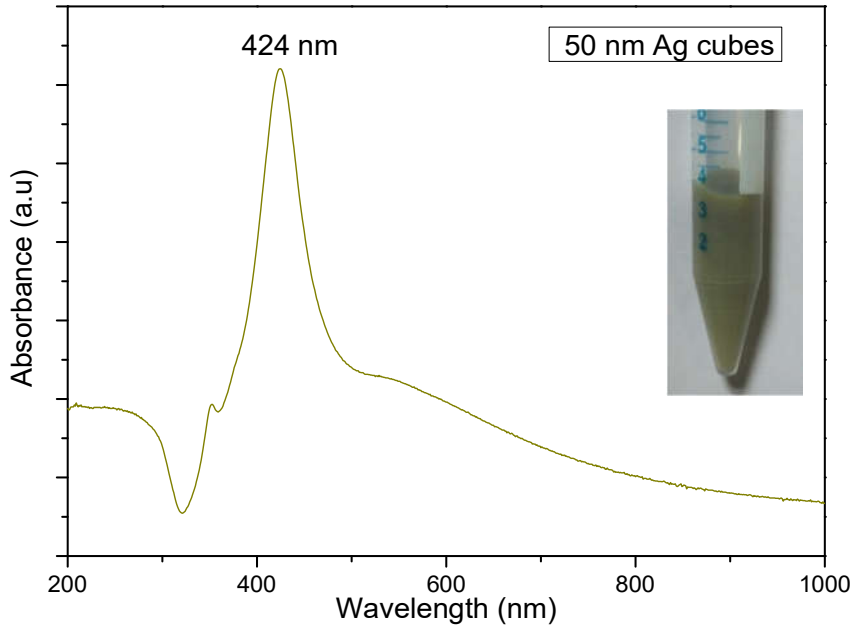

Figure 3.12 : UV-Vis absorption spectrum of silver nanocubes, inset picture of sample

FESEM Images below shows the monodisperse samples of 50 nm sized silver nanocubes

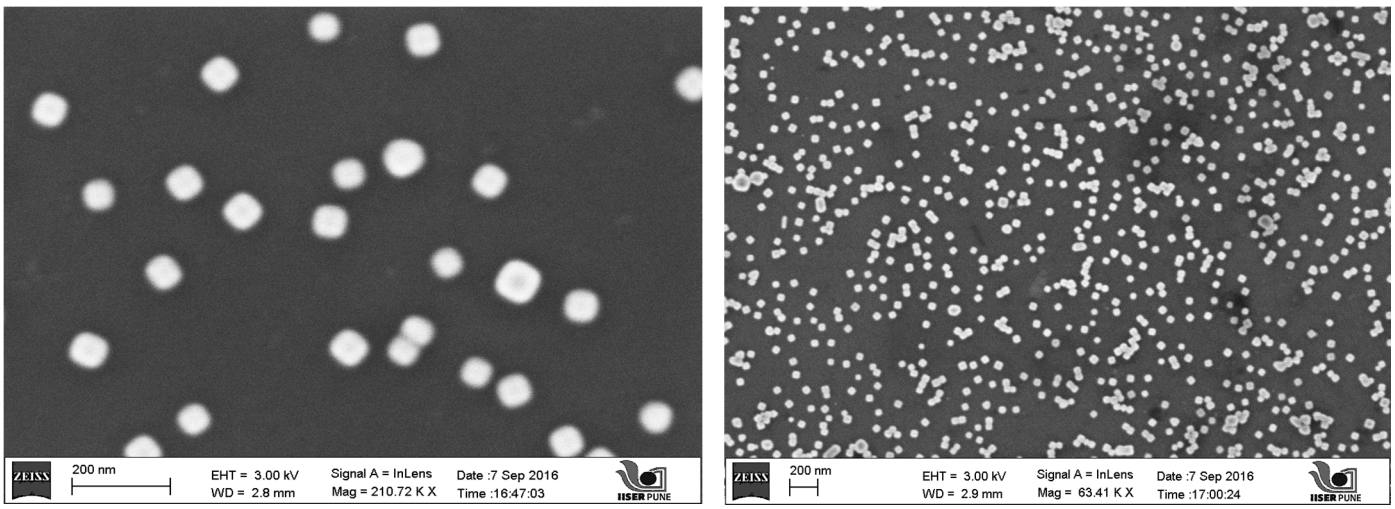

Figure 3.13 : FESEM Images of 50 nm Silver nanocubes

3.1.6 Gold-Silver nanocage

Here following the procedure for the synthesis of cages, addition of gold to the already synthesized silver nanocubes carves out the silver from inside by galvanic displacement and as the amount of gold solution increases the inside becomes more and more hollow to an extent where it is possible to control them till the formation of nanoframes. Further addition will disrupt the whole structure. They are a good in applications where high tuning the plasmonic absorption is required [20].

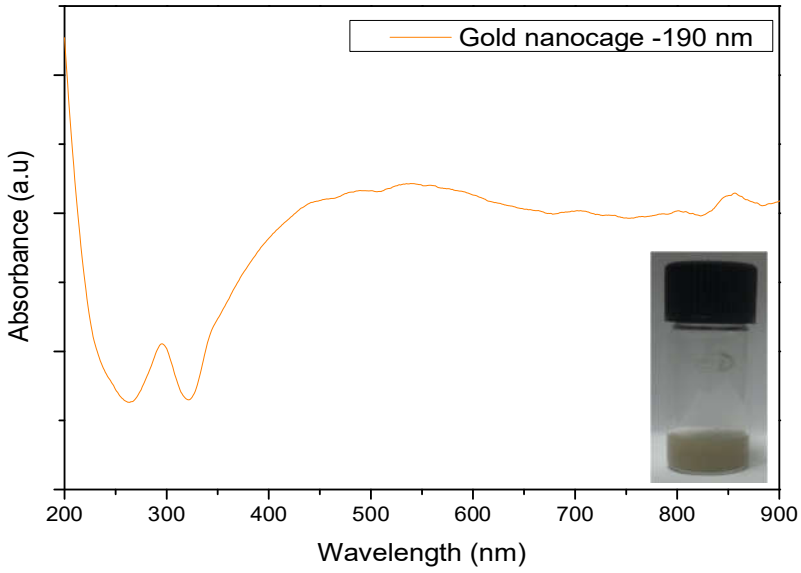

Figure 3.14 : UV-Visible absorption spectrum of gold nanocages of 50nm edge length

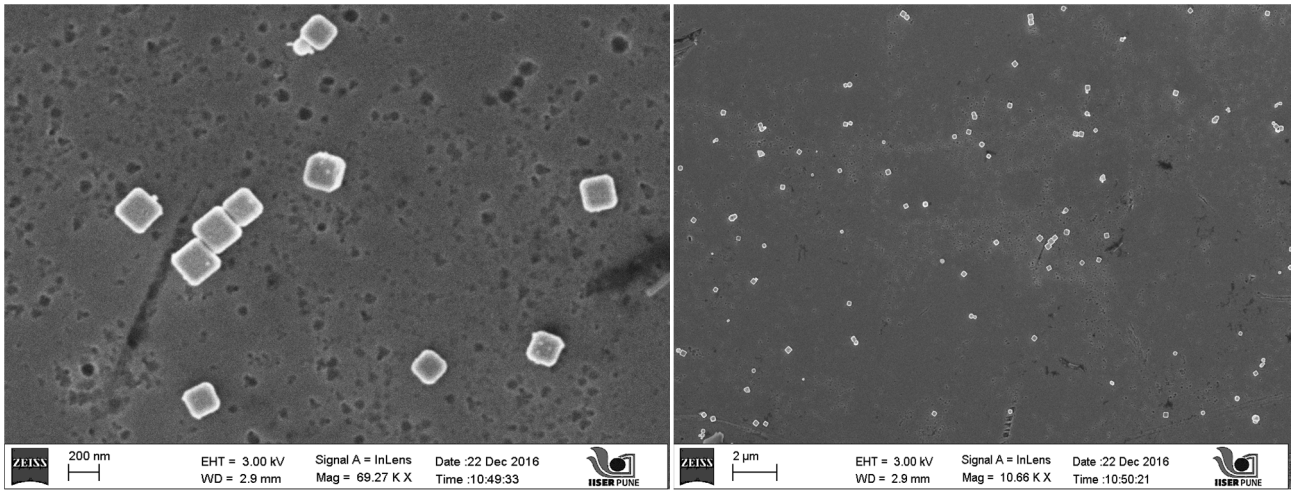

Figure 3.15 : FESEM Images of gold nanocages

TEM Images of Gold nanocages

The transmission electron microscopy images below shows the gold nanocages prepared and discussed above of 190 nm with the addition of 0.3 ml of 1 mM gold solution into the silver nanocube solution prepared by polyol process. Image shows the hole developed on the face of cube through which silver is carved out along with the diffraction images of the cubic faces of silver.

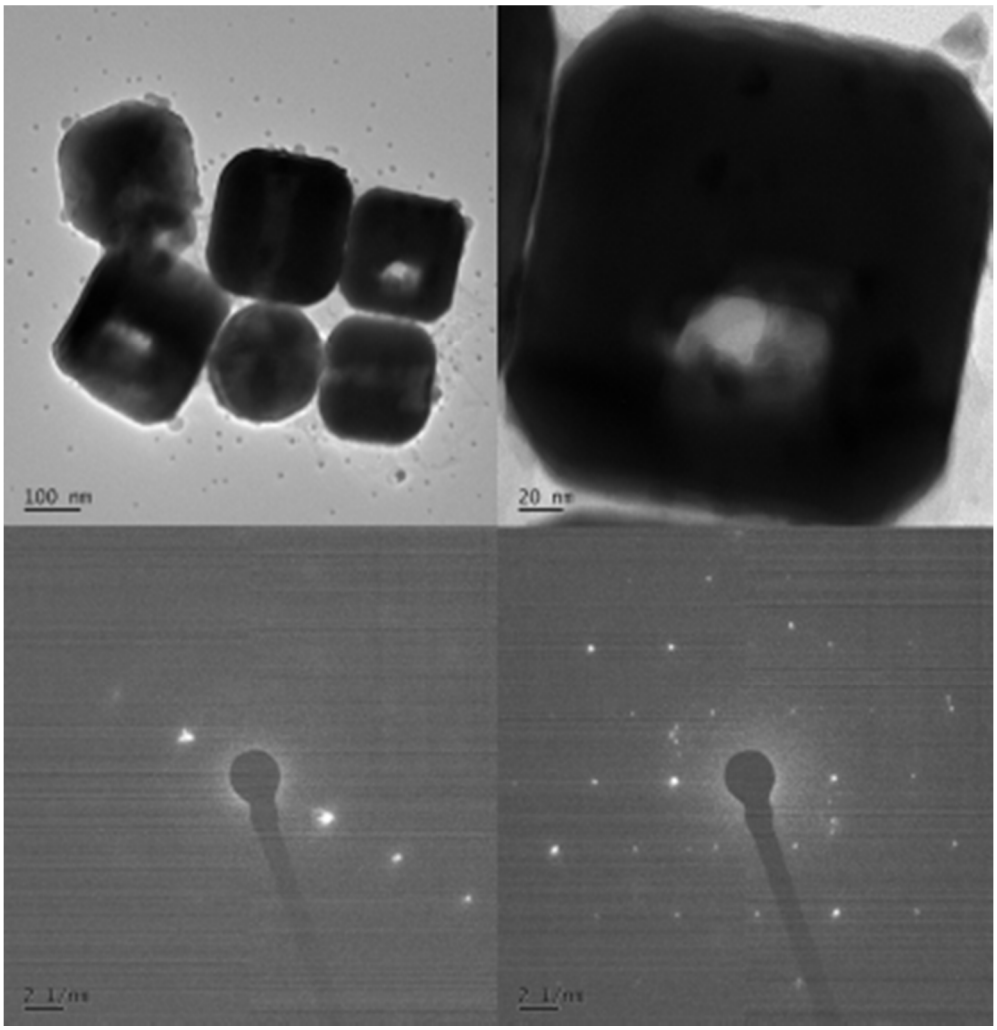

Figure 3.16 : TEM Images of the 190 nm gold nanocages with their diffraction pattern

On addition of further gold solution, silver gets completely carved out of the cube leaving the nanoframe consisting of gold as seen from the TEM images shown below.

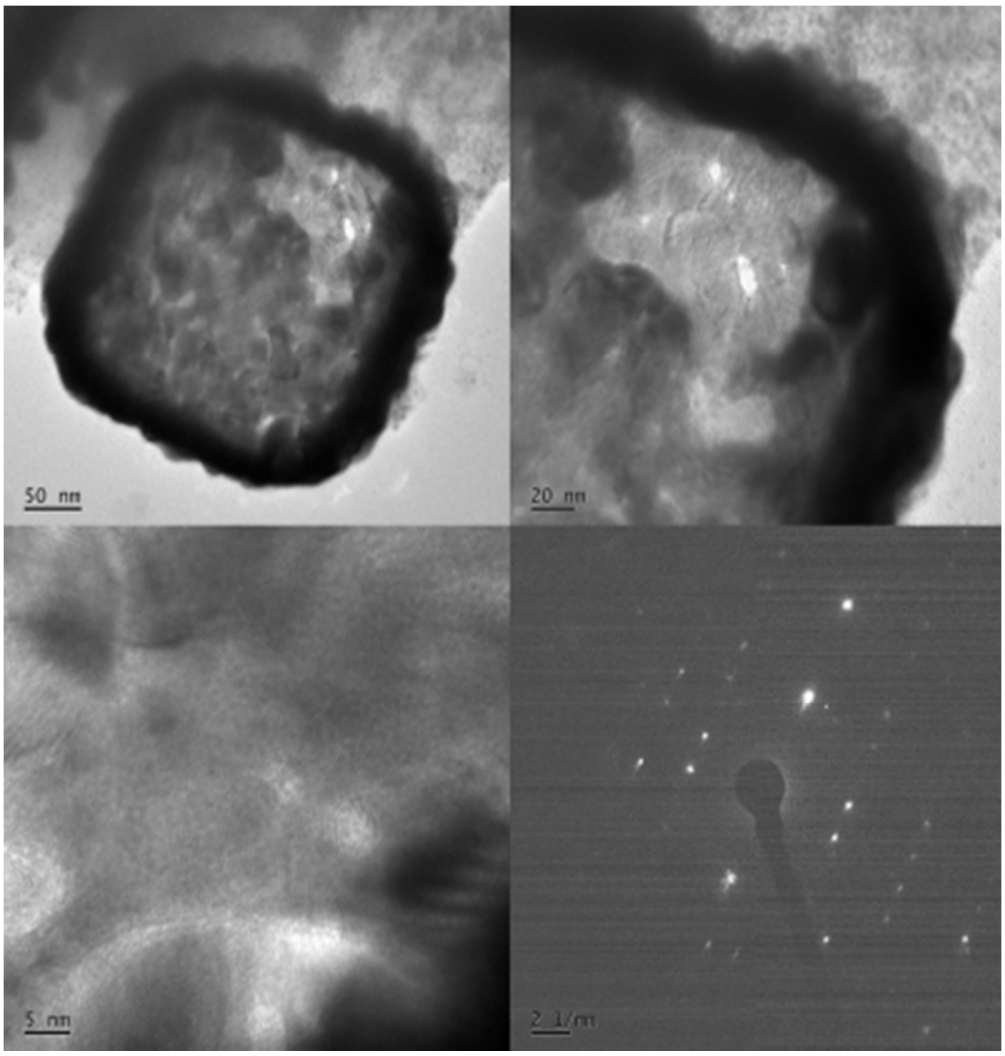

Figure 3.17 : TEM Images of gold nanoframes along with their diffraction pattern

3.2 NPs in PEDOT:PSS

Nanoparticles of various sizes and shapes as discussed above were introduced into the highly conductive polymer PEDOT:PSS as explained in experimental methods of chapter 2. They maintained a ratio of 10 to 40 % volume by volume with the PEDOT:PSS solution. Their properties were characterized by measuring the absorption properties of the solution and transmission and conductivity of the sample by making a thin film by spin coating.

For the spin coating 400 microliters of the actual PEDOT:PSS solution and mixed solutions with varied concentrations of nanoparticles were drop casted on ITO coated glass substrates and spun at 3000 rotations per minute for 30 seconds each. Then they were dried at 120^{o}C under vacuum for 12 hours in vacuum oven.

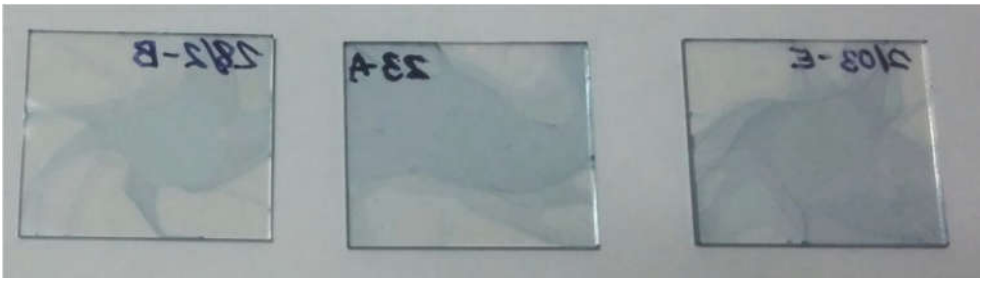

Figure 3.18 : Spin coated films of PEDOT:PSS with NPs incorporated into it on ITO substrate

The slides thus prepared were irradiated under ultraviolet-visible-infrared radiation in solid state spectrophotometer over a range of 300-1000 nm and the resultant spectra were recorded for each.

For the conductivity measurements, contacts are made directly to the films for the I-V characteristics in order to make sure that the conductivity is not compromised on the addition of presence of water as nanoparticles are dispersed in distilled water. Studies are still going on and will be added to the presentations.

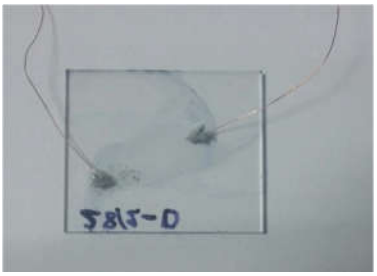

Figure 3.19 : Slide prepared for conductivity measurements on thin film

3.3 Gold nanospheres with PEDOT:PSS

Gold nanospheres (AuNS) of 20 nm size were incorporated into PEDOT:PSS solution in varied concentrations as volume by volume ratio. UV-Vis absorption spectra taken for the samples in order to understand the increased absorption accounted by adding nanoparticles on comparison with the actual PEDOT:PSS polymer solution and the LSPR peaks are at 520 nm.

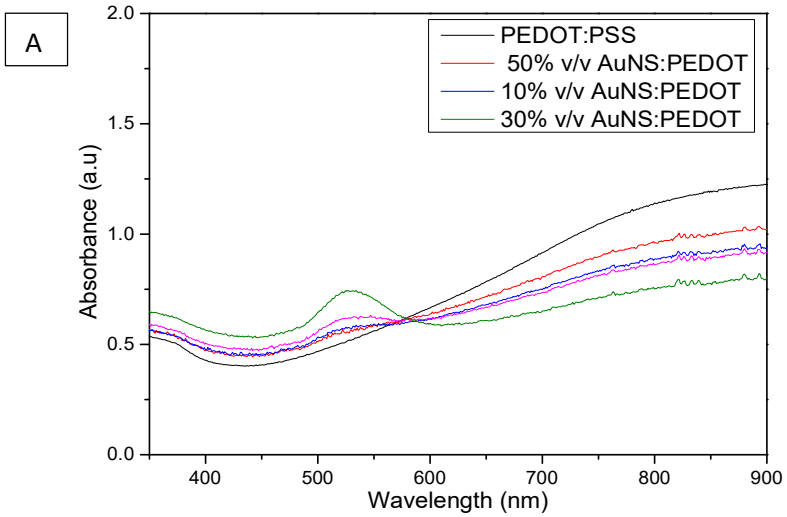

The dip seen in 400 – 500 nm range in the transmission spectra shows the LSPR absorption there and the overall transmission hasn't compromised much on addition of the nanoparticles.

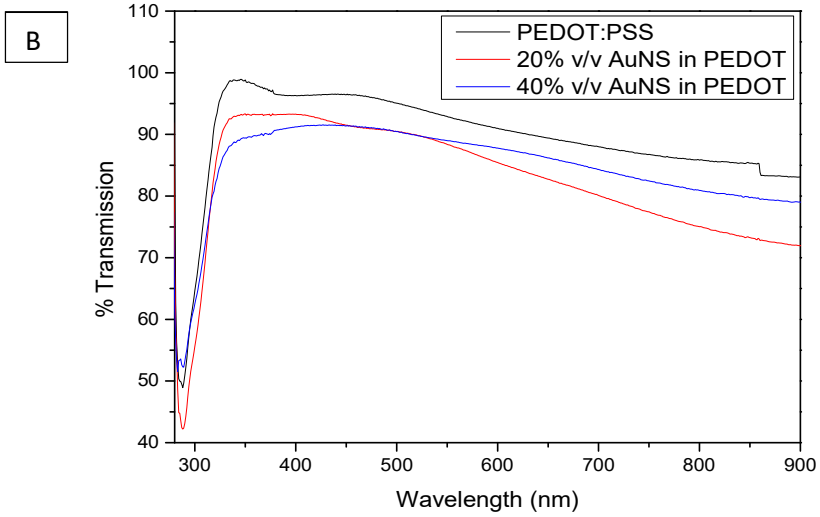

Figure 3.20 : A) UV-Visible absorption spectrum of the solution and B) Transmission spectra of the thin films

The mixture coated substrates were observed under FESEM in order to see the character of the nanoparticles on mixing with the polymer. Images below shows the well dispersed 20 nm gold nanospheres in PEDOT:PSS over 200 nm and 1 μm scale.

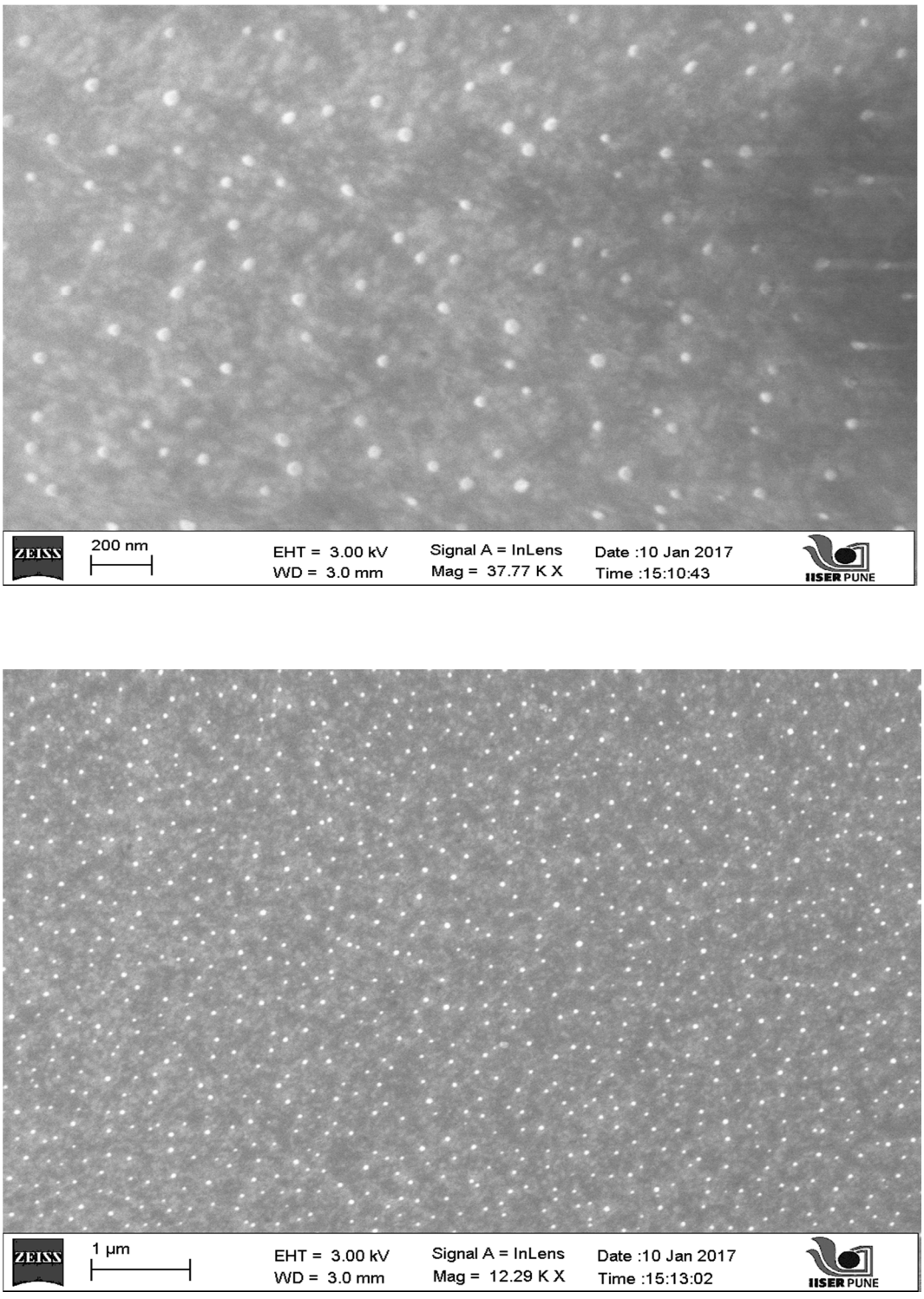

Figure 3.21 : FESEM Images of the thin films of polymer with Au nanospheres

3.4 Gold nanorods with PEDOT:PSS

Nanorods of gold (AuNR) were also incorporated into the polymer PEDOT:PSS in different volume by volume ratios and their absorption properties of solution phase and transmission characteristics of thin films made out of it are shown below. The transmission showed lesser values for the surface plasmon regions of nanorods at their characteristic SP regions as expected.

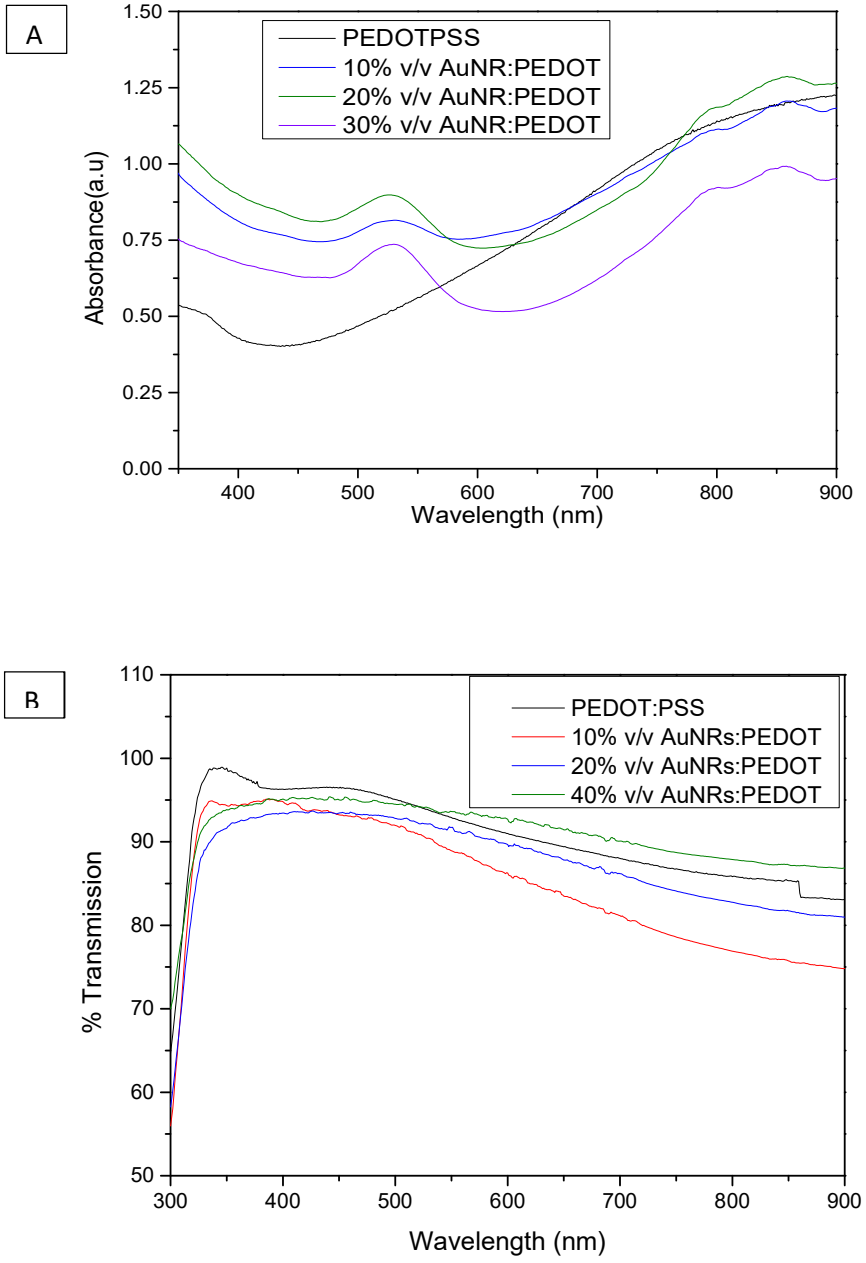

Figure 3.22: A) UV-Visible absorption spectra of the solution and B) transmission spectra of the thin films

3.5 Gold – Copper nanostars with PEDOT:PSS

Gold nanostars (AuStar) on addition to the polymer gave a much higher absorption compared to the other shapes as nanoparticles with sharper edges are bound to show a higher LSPR effect. Reported shapes shows stars with higher power conversion efficiency of 29%[4].

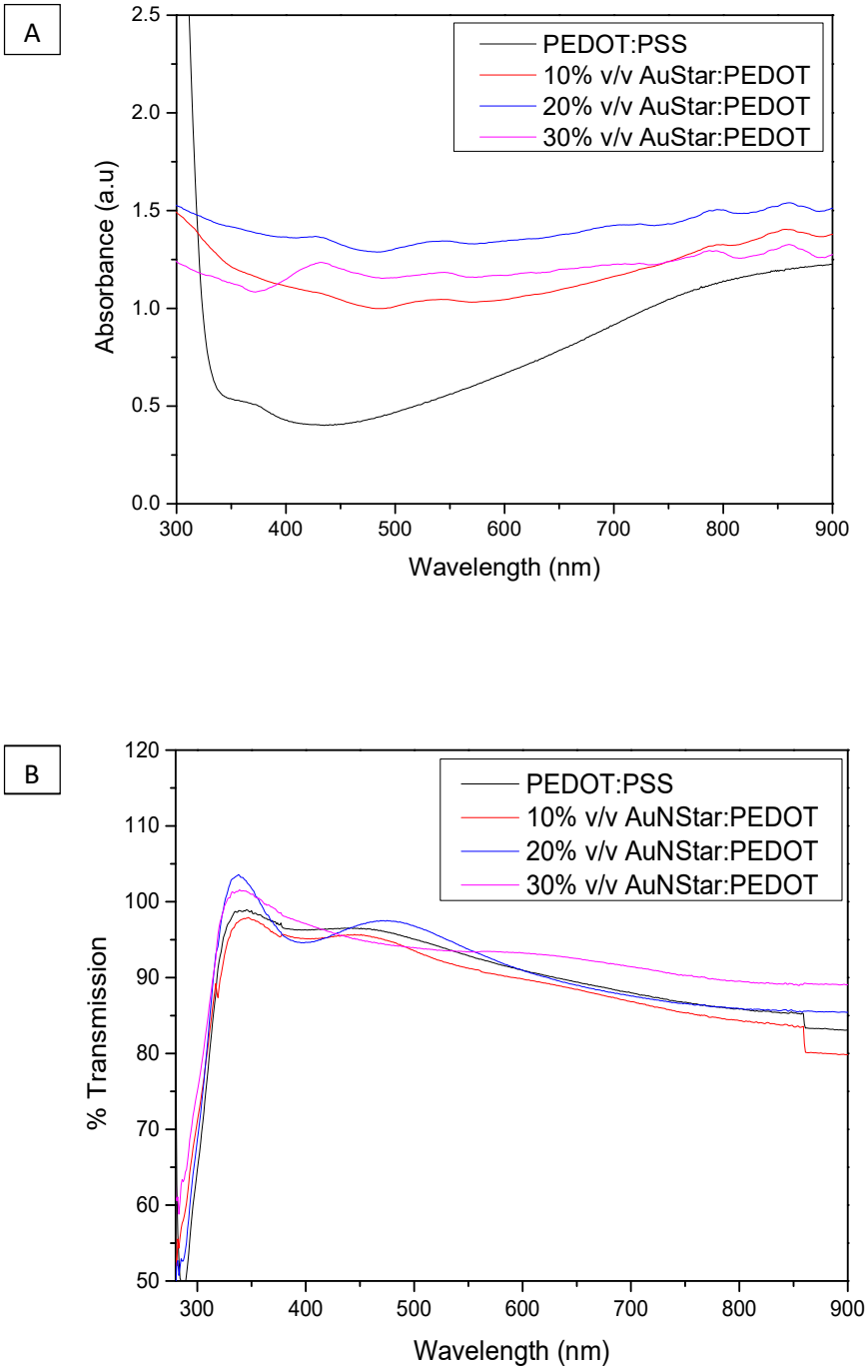

Figure 3.23 : A) UV-Visible absorption spectra of solution and B) transmission spectra of thin films

3.6 Silver nanospheres with PEDOT:PSS

On incorporating with the polymer, 120 nm sized silver nanospheres (AgNS) showed a higher absorption till around 700 nm, which then failed compared to pristine PEDOT solution

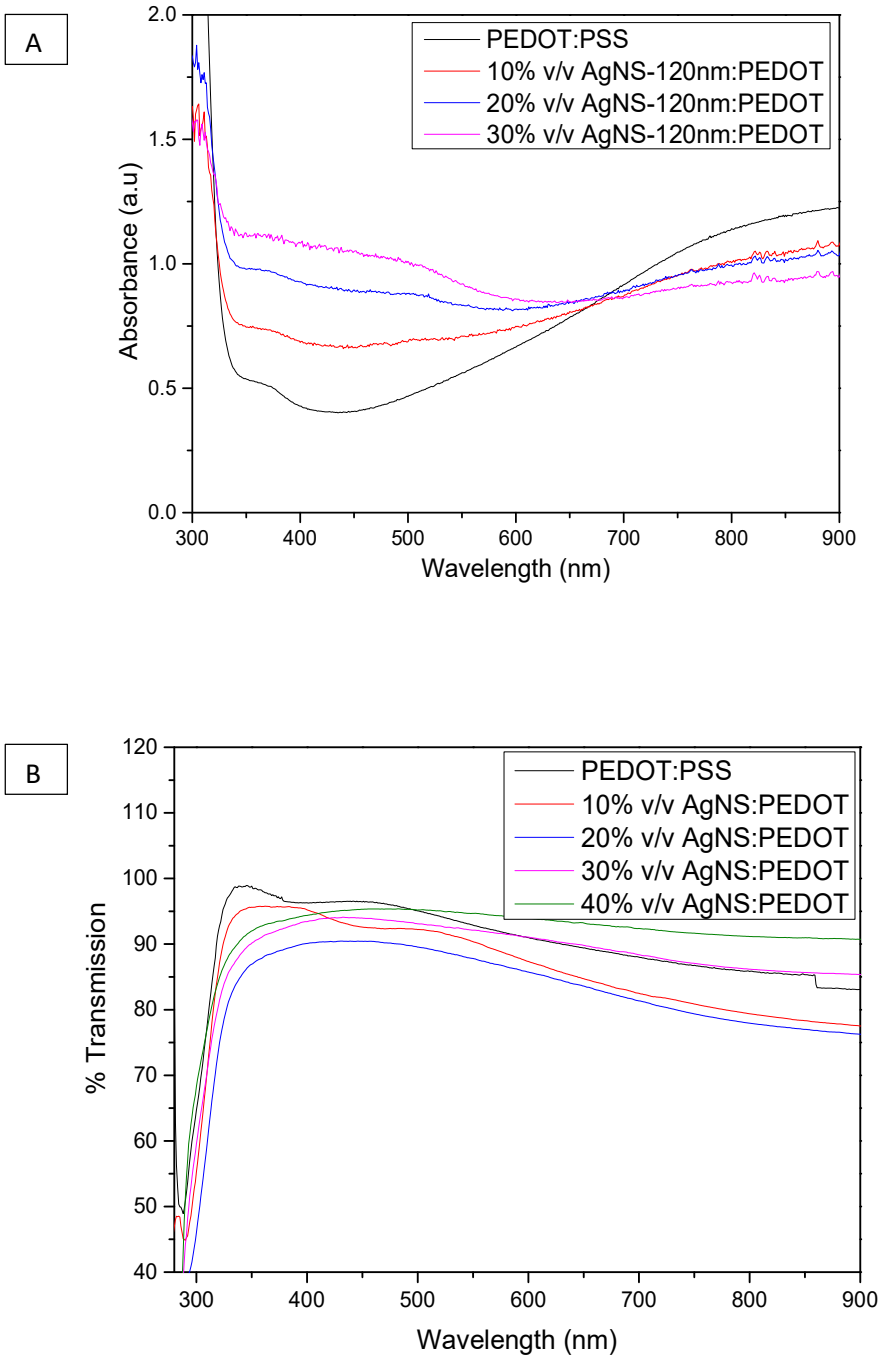

Figure 3.24 : A) UV-Visible absorption spectra of solution and B) transmission spectra of thin films

3.7 Silver cubes with PEDOT:PSS

PEDOT:PSS showed a higher absorption on adding silver nanocubes (AgNC) up to 30% volume by volume. The decreased transmission intensity around 400 nm indicates the SP absorption by the silver nanoparticles.

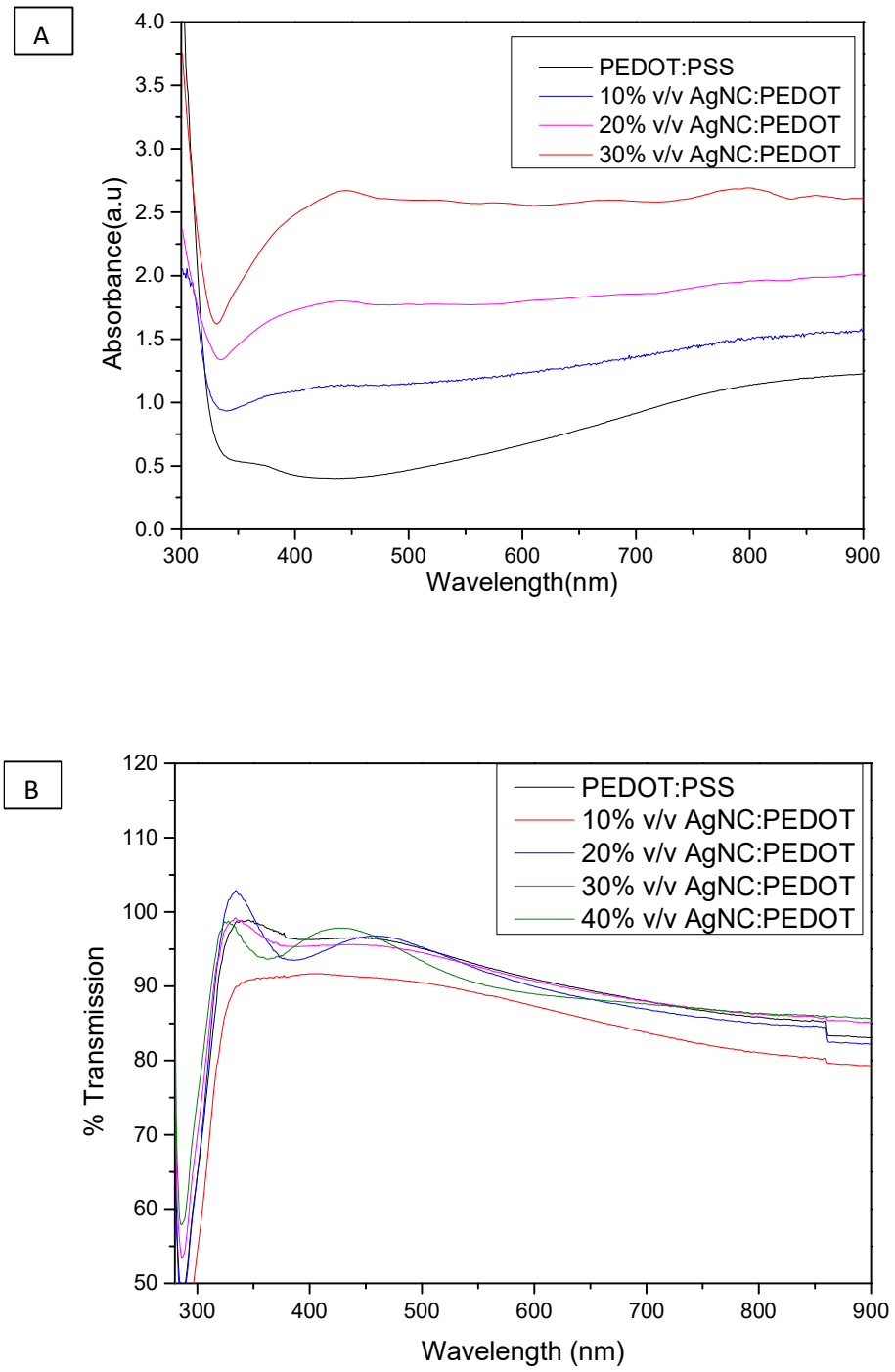

Figure 3.25 : A) UV-Visible absorption spectra of solution and B) transmission spectra of thin films

3.8 50 nm silver nanocubes

Nanocubes of 50 nm edge length also showed a higher absorption on comparison with the pristine PEDOT:PSS as seen in the UV-visible spectrum and a decrease in the transmission range of 400-500 nm shows the SP of silver nanoparticles.

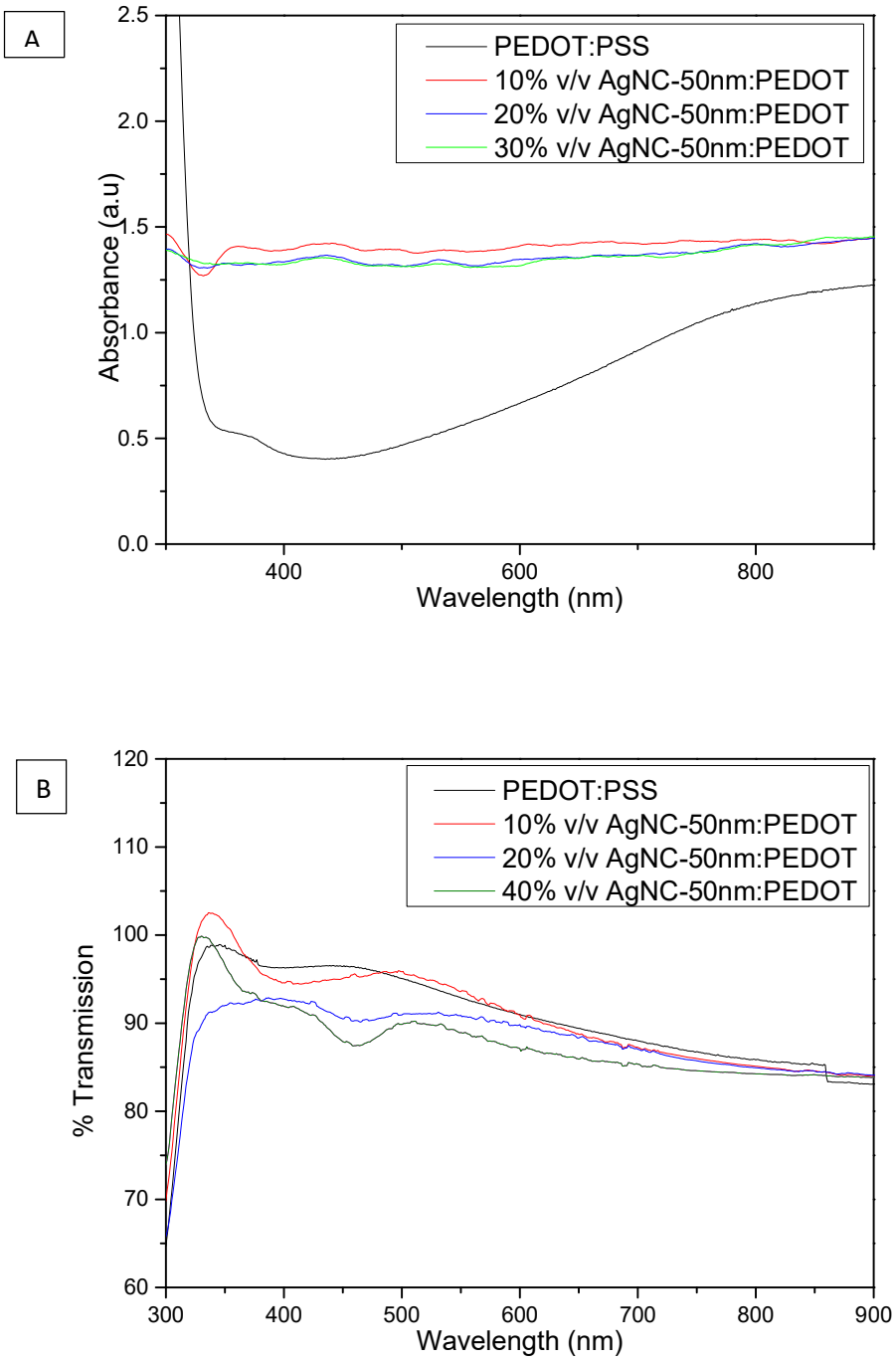

Figure 3.26 : A) UV-Visible absorption spectra of solution and B) transmission spectra of thin films

3.9 Discussion

Plasmonic nanomaterials of two different materials, gold and silver are chosen here in order to compare their properties by light trapping efficiency. Different shapes and sizes gives the perfect tuning to increased absorption by their characteristic localised surface plasmon resonance effects. Like the case of silver nanocubes synthesized have a characteristic LSPR effect of its material, that is silver and due to the cubic shape. Synthesizing cubes of two different sizes as 190 nm and 50 nm here, it is possible to learn the trend of size dependency by comparison.

In order to attain the expected result, the first half of the project was spend on synthesizing nanoparticles of both silver and gold in spheres, rods, cubes and stars. Attaining monodispersity for the synthesized samples was the trickiest part as for the conclusion of results more than 90% of the synthesized sample should be of the expected shapes and size. After much trials of various synthesis methods such as hydrothermal, colloidal and polyol processes followed it was possible to attain much better results for each shape and size made so far. Trials on silver nanorods were done many times following different reported procedure but none seems to attain a rod concentration of not even 50% under analysing through FESEM. A similar thing was happened for the gold nanocubes as well. So a detailed comparison between the materials has to be dropped on those cases due to lack of time. But the rest of the samples as discussed in the starting of third chapter with their UV-visible spectrum and FESEM images over even a micro metre scale clearly indicate the monodispersity of the samples used for the application.

In the next step, they were incorporated into the conducting polymer PEDOT:PSS and blended under ultra sonication. This solution has been examined with UV-visible spectrophotometer and the results above shows the increased absorption after the nanoparticle incorporation compared to the pristine PEDOT:PSS at the region of LSPR effects of individual particles. Then spin coating of each solution on ITO substrates was made at 3000 rpm for 30 seconds each and dried under vacuum at 120^{o}C. These thin films were used for transmission measurements in a range of 300-900 nm. A slight dip is seen in the transmission spectra of the samples around their SP regions showing absorption there but the overall transmission of the prepared films were not compromised much as seen in transmission spectra of each.

The nanoparticles amount are varied in concentration on addition into polymer, as the amount plays an important role in intensifying the electric field around them and in forward scattering light into the active layer. On crossing the amount of optimum nanoparticles required it can actually block the light from going into the next layer. In case of gold nanoparticles, compared to the isotropic gold nanospheres both gold nanorods of 40nm length and nanostars of 200 nm could increase the absorption of light throughout the visible range. Nanoparticles with sharp edges have much stronger LSPR effects compared to the spheres. Even though nanospheres could increase the absorption efficiency till 600 nm range, it failed on extension of range than pristine PEDOT:PSS. For gold nanorods, taking absorptions at particular wavelength of transverse LSPR peak, i.e at 530 nm, incorporation of 10 and 20% v/v rods could increase the absorption by 56 and 72% respectively at that point. Taking the transmission measurements for the slides, pristine PEDOT showed a transmission percentage of ~96% at 450 nm where the incorporation of nanorods hardly decreased it by ~3%. But in case of gold nanostars taking at 430 nm, 10,20 and 30% v/v incorporation increased the absorption of the solutions way higher than 100%, and transmission percentage at 400 nm for the slides prepared with this showed a dip for absorption but did not compromise it more than ~2%.

Taking the case of silver nanoparticles, assuming 90% yield in the synthesis, silver nanospheres have a concentration of 7.9×10^{11} nanoparticles/millilitre, silver nanocubes of 190 nm have 1.26×10^{12} nanoparticles/millilitre and 50 nm silver cubes have 1.3×10^{13} nanoparticles/millilitre. For the silver nanospheres of 120 nm, absorption were increased till 700nm compared to pristine PEDOT:PSS solution. The 50 nm cubes maintained an optimum concentration of 10% in the measured concentrations, with both higher absorption for the solution as well as transmission characteristics for the thin film made with those. In the case of 190 nm cubes a 30% volume by volume ratio could maintain both higher absorption and transmission characteristics. But the conductivity also has to be checked for any compromise in these values due to the water content as particles are dispersed in water. Size and concentration differences leads to the varied optimum concentrations for the optimum device efficiency[4].

Efficiency of a solar cell depends on decreased resistance, increased charge separation and transportation which could be facilitated with the nanoparticles in the polymer layer by changing the morphology of the layer, forward scattering the light into the photo active layer

and their strong LSPR effects. The introduction of more conductive materials into polymer thus enhances the path of holes to electrodes more easily.

3.10 Concluding remarks

In this chapter characterizations of the synthesized nanoparticles are discussed using their UV-Visible spectra and FESEM is discussed. Then proceeded with discussion of the same with the incorporation in highly conductive polymer solution of PEDOT:PSS and their absorption spectra. These solutions are spin coated onto ITO coated glass substrates and dried properly before proceeding onto the transmission measurements of the thin films made. From these data along with the calculated concentrations of nanoparticles in the medium and their size effects their role in increasing the efficiency of such a nanoparticle incorporated layer in photovoltaic cells are discussed. Isotropic nanoparticles here due to their single LSPR peaks, smaller sizes and lesser concentration could not bring the awaited change but the anisotropic particles of larger size had a strong LSPR game with their sharp edges and could scatter more light into the next layer of the cell which is the photoactive layer where the excitons generation and charge separation occurs[6]. Thus anisotropic nanoparticles would be more beneficial.

Transmission measurements are also recorded for each film in order to see whether there is any light blockage by the nanoparticles into the next layer and of course to note down the dip in the spectra near the characteristic absorption range of individual nanoparticles showing the increased absorption at that range of wavelengths.

As the incorporation of different morphologies of gold and silver nanoparticles into the conductive polymer are showing interesting optical and electrical characteristics, organic photovoltaic cells are under construction in a collaboration with IISER Trivandrum group and the priliminary results are found to be promising.

CHAPTER 4

FUTURE WORKS

So far isotropic and anisotropic nanostructures of gold and silver are synthesized, characterized, proceeded with incorporation of the same in conductive polymer PEDOT:PSS and used for the partial construction of a photovoltaic cell till the buffer layer in order to understand the light trapping characters of these nanoparticles. Their effects due to material, size and shapes in the PEDOT:PSS layer are studied using solid state spectrophotometer and FESEM data.

The conductivity measurements and FTIR measurements have to be completed for all the samples/thin films created with each nanoparticle sample in different concentrations of volume by volume ratios in order to have a final say in the efficiency of the photovoltaic cell created with these films as one of the layers. For the gold cage created and analysed in chapter 3, the work with introducing the same into the polymer layer, thin film fabrication and measuring the conductivity measurements is also due.

Bibliography

[1] Ã, H. H. Journal of Quantitative Spectroscopy & Radiative Transfer Gustav Mie and the scattering and absorption of light by particles : Historic developments and basics, *110*, 787–799. (2009).

[2] William Shockley and Hans J. Queisser. Detailed balance limit of efficiency of p-n junction solar cells. *Journal of Applied Physics*, 32:510{519, 1961

[3] J. M. Gee and G. F. Virshup, A 31%-efficient GaAs/silicon mechanically stacked, multijunction concentrator solar cell, *Conference Record of the Twentieth IEEE Photovoltaic Specialists Conference*, Las Vegas, NV, USA, pp. 754-758 vol.1.1988

[4] Kozanoglu D, Apaydin D H, Cirpan A, Esenturk E N. Power Conversion Efficiency Enhancement of Organic Solar Cells By Addition of Gold Nanoparticles, *14*(September), 79. (2012).

[5] Stratakis, E., & Kymakis, E. Nanoparticle-based plasmonic organic photovoltaic devices. *Materials Today*, *16*(4), 133–146. (2013).

[6] Sigma Aldrich site, Organic photovoltaic cells

[7] Woo, S., Jeong, J. H., Lyu, H. K., Han, Y. S., & Kim, Y. In situ-prepared composite materials of PEDOT: PSS buffer layer-metal nanoparticles and their application to organic solar cells. *Nanoscale Research Letters*, *9*(1), 506. (2014).

[8] Stratakis, E., & Kymakis, E. Nanoparticle-based plasmonic organic photovoltaic devices. *Materials Today*, *16*(4), 133–146. (2013).

[9] Sigma Aldrich, Product information of PEDOT:PSS Polymer

[10] Kou, X., Sun, Z., Yang, Z., Chen, H., & Wang, J. Curvature-Directed Assembly of Gold Nanocubes, Nanobranches, and Nanospheres, (26), 1692–1698. (2009).

[11] Apte, A., Bhaskar, P., Das, R., Chaturvedi, S., Poddar, P., & Kulkarni, S. Self-assembled vertically aligned gold nanorod superlattices for ultra-high sensitive detection of molecules. *Nano Research*, *8*(3), 907–919, (2015).

[12] He, R., Wang, Y., Wang, X., Wang, Z., Liu, G., Zhou, W., Hou, J. G. Facile synthesis of pentacle gold–copper alloy nanocrystals and their plasmonic and catalytic properties. *Nature Communications*, *5*, 4327. (2014).

[13] Genc, A., Patarroyo, J., Sancho-Parramon, J., Arenal, R., Duchamp, M., Gonzalez, E. E., Arbiol, J. Tuning the Plasmonic Response up: Hollow Cuboid Metal Nanostructures. *ACS Photonics*, *3*(5), 770–779. (2016).

[14] Liang, H., Wang, W., Huang, Y., Zhang, S., & Wei, H. Controlled Synthesis of Uniform Silver Nanospheres.Pdf, 7427–7431. (2010).

[15] Rustad, L., Peterjohn, W. T., Melillo, J. M., Bowles, F. P., Steudler, P. A., Newkirk, K. M., … Environmental, G. Shape-Controlled Synthesis of Gold and Silver Nanoparticles. *Science*, *298*(December), 2176–2179. (2002).

[16] Skrabalak, S. E., Au, L., Li, X., & Xia, Y. Facile synthesis of Ag nanocubes and Au nanocages. *Nature Protocols*, *2*(9), 2182–2190. (2007).

[17] Chen, F. C., Wu, J. L., Lee, C. L., Hong, Y., Kuo, C. H., & Huang, M. H. Plasmonic-enhanced polymer photovoltaic devices incorporating solution-processable metal nanoparticles. *Applied Physics Letters*, *95*(1), 210–213. (2009).

[18] Hsiao, Y., Charan, S., Wu, F., Chien, F., Chu, C., Chen, P., & Chen, F. Improving the Light Trapping Efficiency of Plasmonic Polymer Solar Cells through Photon Management. (2012).

[19] Kulkarni, S. K. *Nanotechnology : Principles and Practices*. 3rd Ed. Springer. (2014)

[20] Gen A., Patarroyo, J., Sancho-Parramon, J., Arenal, R., Duchamp, M., Gonzalez, E. E., Arbiol, J. Tuning the Plasmonic Response up: Hollow Cuboid Metal Nanostructures. *ACS Photonics*, *3*(5), 770–779. (2016).